General Thermal Conductivity Function for Unsaturated Soils Considering Effects of Water Content, Temperature, and Confining Pressure

Toan Duc Cao, A.M.ASCE[1]; Sannith Kumar Thota, A.M.ASCE[2]; Farshid Vahedifard, F.ASCE[3]; and Amin Amirlatifi[4]

Abstract: The thermal conductivity function (TCF) is an important constitutive function establishing the thermal conductivity–water content relationship in unsaturated soils. The existing TCFs do not account for the effects of confining pressure, nor do they consider thermal induced changes in pore structure and degree of saturation. This study presents a general TCF by considering the temperature effects on pore structure, degree of saturation, different heat transfer mechanisms (i.e., conduction, convection, and latent heat of vaporization), and the confining pressure. The TCF is linked to a temperature-dependent soil water retention curve (SWRC) model to include the impact of temperature on pore structure and degree of saturation. The proposed model applies a decay function to the degree of saturation to account for thermally induced changes in heat transfer mechanisms through conduction and convection of pore water in both liquid and vapor phases and latent heat transfer due to vaporization. A new function is introduced into the TCF to incorporate the effects of confining pressure on thermal conductivity that corresponds to the void ratio changes. The proposed TCF was validated against experimentally measured data for several different soils at zero confining pressure and one soil at various confining pressures reported in the literature. The comparison showed that the proposed TCF can capture laboratory-measured data properly, with prediction errors significantly lower than those from several alternative models. **DOI: 10.1061/(ASCE)GT.1943-5606.0002660.**

Author keywords: Unsaturated soil; Thermal conductivity; Temperature; Heat transfer; Soil water retention curve (SWRC); Confining pressure.

Introduction and Background

Heat transfer in soils is governed by thermal properties, especially thermal conductivity, heat capacity, and thermal diffusivity. The thermal conductivity of soils has a notable influence on many geotechnical and geoenvironmental engineering applications. Examples of such engineering applications include groundwater exploration (Lu and Ge 1996), radioactive waste disposal (Zhang et al. 1994), climate change (Robinson and Vahedifard 2016; Vahedifard et al. 2016a, b, 2017), energy foundation systems (Preene and Powrie 2009; Coccia and McCartney 2012; McCartney et al. 2013; Alsherif and McCartney 2015), and geothermal energy (Ebigbo 2005; Cortes et al. 2009; Yang et al. 2010). Many factors affect the thermal conductivity of unsaturated soils, but these can be separated into three groups (Yun and Santamarina 2008; Jin et al. 2017; McCartney et al. 2019; Yao et al. 2019): (1) index characteristics of soils, including the texture, shape, mineralogy composition, and size; (2) structural conditions, which involve the void ratio and the arrangement of particles; and (3) physical mechanisms such as the effects of water content, temperature, and stress level.

Previous experimental studies (e.g., Gangadhara Rao and Singh 1999; Tarnawski et al. 2009; Zhang et al. 2017) showed that different index characteristics and mineral compositions in soils result in different thermal conductivities. A soil with particles of larger shape and size has higher thermal conductivity (Aduda 1996; Esch 2004; Zhang et al. 2017). Soil with a tighter texture has increased thermal conductivity at given particle sizes (Smith 1942; Sahimi and Tsotsis 1997). Structural conditions representing void ratio and particle arrangement considerably affect the thermal conductivity of soils. For example, soil density is a key factor for heat transfer (Smith 1942; Brandon and Mitchell 1989). A reduction in the void ratio leads to an increase in thermal conductivity (Brandon and Mitchell 1989; Yun and Santamarina 2008). This is because the change in the void ratio affects the quality of interparticle contacts and the pore space.

The magnitude of thermal conductivity in unsaturated soils is controlled by heat transfer within the interparticle contacts and heat loss to the pore space. In terms of dominating physical factors, several experimental results proved that increases in water content increase the thermal conductivity (Chen 2008; Tarnawski et al. 2013;

[1]Adjunct Professor, Dept. of Civil Engineering Technology, Environmental Management and Safety, Rochester Institute of Technology, NY 14623; formerly, Postdoctoral Research Associate, Center for Advanced Vehicular Systems (CAVS) and Richard A. Rula School of Civil and Environmental Engineering, Mississippi State Univ., Mississippi State, MS 39762. Email: tdcite@rit.edu

[2]Senior Staff Engineer, Schnabel Engineering, 46020 Manekin Plaza #150, Sterling, VA 20166; formerly, Ph.D. Candidate, Richard A. Rula School of Civil and Environmental Engineering, Mississippi State Univ., Mississippi State, MS 39762. Email: sannyy21@gmail.com

[3]Civil and Environmental Engineering (CEE) Advisory Board Endowed Professor and Professor, Richard A. Rula School of Civil and Environmental Engineering, Mississippi State Univ., Mississippi State, MS 39762 (corresponding author). ORCID: https://orcid.org/0000-0001-8883-4533. Email: farshid@cee.msstate.edu

[4]Assistant Professor, Swalm School of Chemical Engineering, Mississippi State Univ., Mississippi State, MS 39762. Email: amin@che.msstate.edu

Note. This manuscript was submitted on June 23, 2020; approved on June 30, 2021; published online on August 30, 2021. Discussion period open until January 30, 2022; separate discussions must be submitted for individual papers. This paper is part of the ***Journal of Geotechnical and Geoenvironmental Engineering***, © ASCE, ISSN 1090-0241.

Lu and Dong 2015; Jin et al. 2017; Zhang et al. 2017) because the flow of water, in liquid and vapor forms, directly affects the heat transfer. Furthermore, the thermal conductivity of unsaturated soils increases as the confining pressure increases (e.g., Vargas and McCarthy 2001; Yun and Santamarina 2008; Yao et al. 2019) because the confining pressure results in higher packing density and trapping of small particles between the larger pore spaces. This also reduces the void ratio of soil due to the rearrangement of particles. Temperature is another physical factor dominating the thermal conductivity in unsaturated soils. Because changes in the temperature affect pore structure, degree of saturation, and heat transfer mechanisms, it plays a significant role in the magnitude of thermal conductivity in unsaturated soils (e.g., de Vries 1963; Johansen 1975; Kasubuchi 1992; Kasubuchi and Hasegawa 1994; Campbell et al. 1994; Smits et al. 2013; Moradi et al. 2016; Yao et al. 2019).

Over the last few decades, several attempts have been made to develop analytical models to describe the thermal conductivity function (TCF), which establishes a constitutive function between the thermal conductivity and water content (or suction) in soils. Several articles in the literature comprehensively reviewed most of these TCFs (e.g., Dong et al. 2015; Zhang and Wang 2017; Zhang et al. 2017). The first TCF can be credited to de Vries (1963), who proposed mathematical models for determining the thermal conductivity of soils based on their physical properties. The advantage of the de Vries model is that a fitting parameter is not needed. Campbell et al. (1994) and Tarnawski et al. (2000a, b) investigated temperature effects on thermal conductivity of unsaturated soils. Slavin et al. (2000) defined a model to determine the thermal conductivity of solid spherical particles immersed in a static fluid. Hu et al. (2001) and Gori and Corasaniti (2002) employed capillary pressure–saturation relationships to develop TCFs for an unconsolidated porous medium under temperature effects. Côté and Konrad (2005) and Lu et al. (2007) utilized a sigmoidal shape to model the TCF controlled by an empirical fitting parameter based on the effects of grain size, pore size, and pore water. Haigh (2012) and Dong et al. (2015) presented TCFs based on the assumption of perfectly spherical soil grains to match experimental data of the curved shape of thermal conductivity–water content for binary mixtures. Lu and Dong (2015) provided a model that employs two soil-specific parameters, soil particles and the pore fluid network connectivity, within the funicular regime. Wallen et al. (2016) used the Lu and Dong (2015) model to analyze the thermal conductivity of binary sand mixtures with different degrees of saturation. Zhang et al. (2017) developed a TCF by considering the effect of water content, dry density, particle size, and mineral composition. Samarakoon and McCartney (2019) developed a model by considering the temperature effects on thermal conductivity that emerge from heat transfer by conduction and convection while ignoring its effects on pore-fluid properties. They introduced two fitting parameters to account for vapor diffusion.

Although several TCFs have been proposed in the literature, gaps remain to be filled regarding the development of a general TCF that can account for all, or the majority of, dominating physical mechanisms of the thermal conductivity of unsaturated soils. For example, the existing TCFs do not account for the effects of confining pressure, nor do they consider thermal induced changes in pore structure and degree of saturation. To fill this gap, this study proposes a new TCF for unsaturated soils by considering the temperature effects on pore structure, degree of saturation, different heat transfer mechanisms (i.e., conduction, convection, and latent heat of vaporization), and the confining pressure. A parametric analysis was conducted of the proposed TCF to illustrate changes in the thermal conductivity of three different soils under temperatures ranging from 25°C to 80°C and confining pressures ranging from 0 to 300 kPa. The accuracy of the proposed model was evaluated by comparing it with several sets of experimental data and alternative models available in the literature.

Model Development and Analytical Derivation

Underlying Theory and General Functional Form

Fig. 1 schematically shows the conceptual model used to develop TCF in this study. To account for various factors affecting the thermal conductivity of unsaturated soils, the proposed TCF is constituted by considering three distinct yet interrelated factors:

- TCF is linked to the soil water retention curve (SWRC), accounting for two main water storage mechanisms (i.e., capillary and adsorption). Because water has higher thermal conductivity than dry soil or air, the higher the water content, the higher is the thermal conductivity.
- The impact of temperature is another important factor affecting the thermal conductivity of unsaturated soils, through convective water-vapor flow and phase changes or latent heat transfer (e.g., de Vries 1987; Campbell et al. 1994; Tarnawski and Gori 2002; Smits et al. 2013; Moradi et al. 2016; Xu et al. 2019).
- Changes in confining pressure impose variation of thermal conductivity of unsaturated soils due to the internment of pore network and soil particles (e.g., Yun and Santamarina 2008; Yao et al. 2014, 2019).

This study presents a general TCF based on the aforementioned primary factors (Fig. 1). The proposed model was established by considering the temperature effects on thermal conductivity by linking the TCF to a temperature-dependent SWRC (Vahedifard et al. 2018), which can capture the effect of temperature on capillary and adsorbed water, in which the capillary part accounts for the temperature effects on enthalpy, contact angle, and surface tension [Fig. 1(a)]. Furthermore, the TCF accounts for the effect of elevated temperatures on heat transfer mechanisms through a decay function [Fig. 1(b)]. Based on the concept shown in Fig. 1(c), the effect of confining pressure on the TCF also is taken into account. The general TCF for unsaturated soils can be expressed as:

$$\lambda = \lambda^{\text{Base}} + \Delta\lambda^{\text{CP}} + \Delta\lambda^{\text{HM}} \tag{1}$$

where λ = total thermal conductivity; λ^{Base} = base thermal conductivity; $\Delta\lambda^{\text{HM}}$ = change in thermal conductivity induced by temperature effect on heat transfer mechanisms; and $\Delta\lambda^{\text{CP}}$ = change in thermal conductivity due to effects of confining pressure. In the proposed model, the base model concurrently accounts for variations of water content and temperature and is linked to the temperature-dependent SWRC. That is

$$\lambda^{\text{Base}} = \lambda^{\text{TSWR}} \tag{2}$$

where λ^{TSWR} is the base thermal conductivity linked to the temperature-dependent SWRC to account for the effect of water content while incorporating the temperature effect on pore structure and degree of saturation.

Water Content–Temperature Effects on Thermal Conductivity

Linkage to Temperature-Dependent SWRC

Several studies have demonstrated the linkage between the TCF and the SWRC, which allows accounting for the effect of water content (or suction) on the thermal conductivity of unsaturated soils (e.g., Côté and Konrad 2005; Lu and Dong 2015). The SWRC,

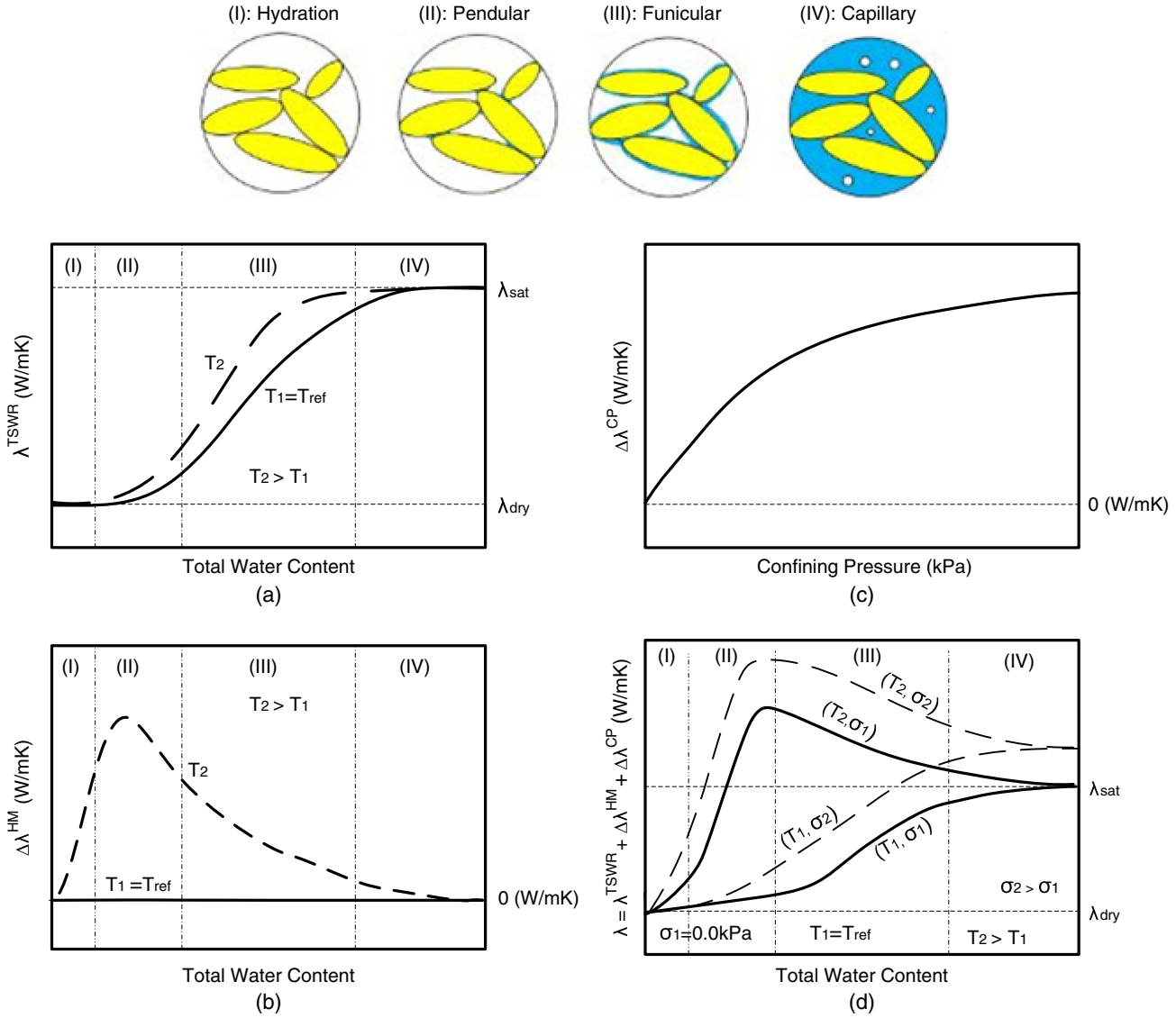

Fig. 1. Generalized thermal conductivity function for unsaturated soils: (a) λ^{TSWR}, base thermal conductivity linked to the temperature-dependent SWRC to account for the effect of temperature on pore structure and degree of saturation; (b) $\Delta\lambda^{HM}$, change in thermal conductivity induced by the temperature effect on heat transfer mechanisms; (c) $\Delta\lambda^{CP}$, change in thermal conductivity due to the effects of confining pressure; and (d) λ, total thermal conductivity ($\lambda = \lambda^{TSWR} + \Delta\lambda^{HM} + \Delta\lambda^{CP}$).

defined as a relationship between the matric suction and water content, may have four different desaturation stages based on capillarity and adsorption mechanisms of the soil (Fig. 1). These generally are categorized as (1) hydration, which refers to the water attracted by intermolecular forces by van der Waals, electrical, osmotic, and hydration components; (2) pendular or discontinuous water phase, in which the water forms menisci near particles; (3) funicular or continuous water phase, in which menisci are interconnected with each other (e.g., Cho and Santamarina 2001; Lu and Dong 2015); and (4) capillary, in which the air phase is in the form of bubbles (Lu and Likos 2004, 2006). Considering these four soil water retention regimes (Fig. 1), the thermal conductivity changes distinctly as the water content changes from one to another retention regime (e.g., Johansen 1975; Côté and Konrad 2005; Lu et al. 2007; Dong et al. 2015; Lu and Dong 2015). Considering this aspect, Lu and Dong (2015) proposed a TCF using a sigmoidal function of the pore fluid network connectivity parameter, m, and the total water content at ambient conditions as

$$\lambda = \lambda_{sat} - (\lambda_{sat} - \lambda_{dry})\left[1 + \left(\frac{\theta}{\theta_f}\right)^m\right]^{(1-m)/m} \quad (3)$$

Or, in terms of the degree of saturation, S, as

$$\lambda = \lambda_{sat} - (\lambda_{sat} - \lambda_{dry})\left[1 + \left(\frac{S}{S_f}\right)^m\right]^{(1-m)/m} \quad (4)$$

where λ_{sat} and λ_{dry} = thermal conductivity at saturated and dry states, respectively; θ_f and S_f = volumetric water content and degree of saturation at which funicular regime starts; and m = pore fluid network connectivity parameter for thermal conductivity. Lu and Dong (2015) showed that θ_f, S_f, and m are linearly correlated to the residual water content (θ_r), residual degree of saturation (S_r), and fitting parameter (n_{VG}), respectively, of the van Genuchten (1980) SWRC model.

Johansen (1975) proposed empirical formulations to estimate λ_{sat} and λ_{dry} using index properties of soils as

$$\lambda_{\text{dry}} = \frac{0.135\rho_d + 0.0647}{\rho_p - 0.947\rho_d} \tag{5}$$

$$\lambda_{\text{sat}} = \lambda_S^{1-n}\lambda_w^n \tag{6}$$

$$\lambda_s = \lambda_q^q \lambda_o^{1-q} \tag{7}$$

where ρ_p = particle density; ρ_d = dry density; λ_s = effective thermal conductivity of soil solids; λ_w = thermal conductivity of water (0.594 $\text{W m}^{-1}\text{ K}^{-1}$); λ_q = thermal conductivity of quartz [7.69 $\text{W m}^{-1}\text{ K}^{-1}$ (Campbell et al. 1994)]; q = quartz content of total solids; and λ_o = thermal conductivity of other minerals (2.0 $\text{W m}^{-1}\text{ K}^{-1}$).

Considering the intrinsic linkage between the TCF and the SWRC, and to account for the effect of temperature, the TCF of Lu and Dong (2015) was extended by incorporating the temperature-dependent SWRC model developed by Vahedifard et al. (2018, 2019). The temperature-dependent SWRC model accounts for the effect of temperature on capillarity and adsorption. Thermally induced changes in capillary pressure (commonly referred to as matric suction) can be captured by quantifying the temperature dependency of surface tension, contact angle, and enthalpy of immersion (Vahedifard et al. 2018, 2020). If the wetting coefficient, enthalpy, and water–air surface tension are functions of temperature, the temperature-dependent matric suction can be determined as (Grant and Salehzadeh 1996)

$$\psi = \psi_{T_r}\left(\frac{\beta + T}{\beta_{T_r} + T_r}\right) \tag{8}$$

where $\psi = u_a - u_w$ = matric suction at arbitrary temperature T (K); ψ_{T_r} = matric suction at arbitrary reference temperature T_r; u_a = pore-air pressure; u_w = pore-water pressure; and β is calculated as (Grant and Salehzadeh 1996)

$$\beta = \frac{-\Delta h T_r}{-\Delta h + a'(\cos\alpha)_{T_r} + b(\cos\alpha)_{T_r} T_r} \tag{9}$$

where α = temperature-dependent contact angle; and Δh = enthalpy of immersion per unit area. The enthalpy is determined through experimental measurements or differential enthalpy of the vapor's adsorption (Everett 1972; Vahedifard et al. 2020). A reduction of the enthalpy by increasing temperature, as suggested by Watson (1943), is considered as

$$\Delta h = \Delta h_{T_r}\left(\frac{1 - T_r}{1 - T}\right)^{0.38} \tag{10}$$

where Δh_{T_r} = enthalpy of immersion per unit area at reference temperature.

Eqs. (8)–(10) can be employed to extend the SWRC model of van Genuchten (1980) to temperature-dependent conditions. The total water content given by the van Genuchten (1980) SWRC model under ambient temperature is

$$\theta = \theta_a + (\theta_s - \theta_a)(1 + (\alpha_{VG}\psi)^{n_{\text{VG}}})^{-m_{\text{VG}}} \tag{11}$$

where θ, θ_s, and θ_a = total water content, saturated water content, and adsorbed water content, respectively; α_{VG} = fitting parameter inversely related to air-entry suction (1/kPa); and m_{VG} = fitting parameter representing overall geometry of SWRC, commonly assumed to be $m_{\text{VG}} = 1 - 1/n_{\text{VG}}$. The full expression of the temperature-dependent SWRC model is (Grant and Salehzadeh 1996; Lu 2016; Vahedifard et al. 2018)

$$\theta = \theta_a^{\max}\left\{\exp\left[\frac{-M_w\psi\left(\frac{\beta_{T_r}+T_r}{\beta+T}\right)}{RT}\right]\right\}^{1/M} + \frac{\theta_s - \theta_a^{\max}}{\left\{1 + \left[\alpha_{\text{VG}}\psi\left(\frac{\beta_{T_r}+T_r}{\beta+T}\right)\right]^{n_{VG}}\right\}^{1/n_{\text{VG}}-1}} \times \left\{\exp\left[\frac{-M_w\psi\left(\frac{\beta_{T_r}+T_r}{\beta+T}\right)}{RT}\right]\right\}^{1/M} \tag{12}$$

where $\theta_a^{\max}$ = adsorption capacity; $M_w = 1.8 \times 10^{-5}$ $\text{m}^3\text{ mol}^{-1}$ = molar volume of water; $R = 8.314$ $\text{J mol}^{-1}\text{ K}^{-1}$ = universal gas constant; and M = adsorption strength, which is a fitting parameter controlled by mineral type and quantity. A key feature of the extended van Genuchten SWRC model is that the formulation needs only the SWRC fitting parameters at the ambient temperature, and Δh_{T_r} is the sole additional parameter needed to account for the effect of temperature.

By substituting the water content obtained from the extended van Genuchten model [Eq. (12)] into Eqs. (3) or (4), respectively, one can extend the Lu and Dong (2015) model to temperature-dependent conditions and determine λ^{TSWR} in terms of water content as

$$\lambda^{\text{TSWR}} = \lambda_{\text{sat}} - (\lambda_{\text{sat}} - \lambda_{\text{dry}}) \times \left[1 + \left(\frac{\theta_a}{\theta_f} + \frac{(\theta_s - \theta_a)}{\theta_f}\left(1 + \left(\alpha_{\text{VG}}\psi\left(\frac{\beta_{T_r} + T_r}{\beta + T}\right)\right)^{n_{\text{VG}}}\right)^{1/n_{\text{VG}}-1}\right)^m\right]^{(1-m)/m} \tag{13}$$

Or, in terms of the degree of saturation

$$\lambda^{\text{TSWR}} = \lambda_{\text{sat}} - (\lambda_{\text{sat}} - \lambda_{\text{dry}})\left[1 + \left(\frac{S_a}{S_f} + \frac{(1 - S_a)}{S_f}\left(1 + \left(\alpha_{\text{VG}}\psi\left(\frac{\beta_{T_r} + T_r}{\beta + T}\right)\right)^{n_{\text{VG}}}\right)^{1/n_{\text{VG}}-1}\right)^m\right]^{(1-m)m} \tag{14}$$

where S_a = degree of saturation of adsorbed water. To illustrate the dependency of λ^{TSWR} on the temperature-dependent SWRC, the proposed equations were solved using the input parameters in Table 1; Δh_{T_r} values were reported for similar soils by Grant and Salehzadeh (1996), and all other parameters were obtained from Lu (2016) and Lu and Dong (2015).

Figs. 2(a–c) illustrate the total water content versus matric suction for Georgia kaolinite, Bonny silt, and Ottawa sand, respectively, subjected to temperatures from 25°C to 80°C. For a given suction, a higher temperature led to lower water content. This reduction can be attributed to changes in surface tension, contact angle, and enthalpy (Vahedifard et al. 2018). The results show that the

Table 1. SWRC and TCF parameters of three soils used in parametric study

	SWRC parameters[a]						Thermal parameters[b]			
Soil	θ_s	M	n_{VG}	α_{VG} (kPa^{-1})	Δh_{T_r} (Jm^{-2})	θ_a^{max}	λ_{sat} ($W\,m^{-1}\,K^{-1}$)	λ_{dry} ($W\,m^{-1}\,K^{-1}$)	m	θ_f
Georgia kaolinite	0.57	0.047	1.42	0.008	−0.516	0.043	1.56	0.24	2.92	0.087
Bonny silt	0.47	0.049	1.43	0.050	−0.516	0.020	1.28	0.37	2.62	0.062
Ottawa sand	0.40	0.789	4.50	0.282	−0.285	0.017	2.50	0.23	1.93	0.032

[a]Reported in Lu (2016), except Δh_{T_r}, which is taken from Grant and Salehzadeh (1996).
[b]Reported in Lu and Dong (2015).

effect of temperature for matric suctions higher than 10,000 kPa for Georgia kaolinite and 100 kPa for Bonny silt became less significant. For Ottawa sand, the matric suction varied between 0 and 10 kPa [Fig. 1(c)]. At such low matric suctions, capillarity is the dominant water storage mechanism, and adsorption has less effect.

The effect of changes in water content and temperature sensitivity on λ^{TSWR} is depicted in Figs. 2(d–f) for Georgia kaolinite, Bonny silt, and Ottawa sand, respectively. The trend for all three soils generally was affected by temperature-induced changes in matric suction and total water content. Therefore, λ^{TSWR} for all soils due to higher temperatures was affected by the water retention mechanisms [Figs. 2(a–c)]. For all three soils, λ^{TSWR} exhibited a monotonic increase and then became constant for temperatures ranging from 25°C to 80°C. For each temperature, the increasing trend of λ^{TSWR} continued as long as the water content (or matric suction) varied within the capillary regime. For all soils at a given water content, the increase in temperature enhanced the thermal conductivity. On the other hand, for both dry and saturated conditions, the temperature dependence of thermal conductivity was negligibly small. As water content increases with temperature, there is enhanced heat conduction through water and soil particles because they are superior in conducting heat to the air medium. At relatively low water content, the soil has air pores; therefore, λ^{TSWR} decreases.

The thermally induced increase in thermal conductivity is because the temperature significantly affects the menisci of the water bridges (liquid–solid) of particles, which leads to more air space between particles provided by the reduction of water content up to the funicular water content. Beyond the funicular water content, the air becomes continuous and water meniscus becomes discontinuous, hence further decreasing the thermal conductivity but at a slower rate until reaching the dry region, in which the temperature does not have much influence on λ^{TSWR}. The peak of thermal conductivity is higher for coarse-grained soils such as sand [Fig. 2(f)] than for fine-grained soils [Figs. 2(d and e)]. This could be because coarse particles, due to the absence of heat resistance, conduct heat better than do fine particles. These observations are consistent with the laboratory test results reported in the literature (e.g., Hiraiwa and Kasubuchi 2000; Smits et al. 2013; Xu et al. 2016).

For comparison, to evaluate the thermal conductivity near the dry and near saturated states, the percentage change of thermal conductivity with temperature was calculated for all three soils at water contents of 0.1 and 0.3. At the low water content of 0.1, the increase in λ^{TSWR} for Georgia kaolinite [Fig. 2(d)] was approximately 22%, 39%, and 53% as the temperature increased from 25°C to 40°C, 60°C, and 80°C. For Bonny silt [Fig. 2(e)], the increase in λ^{TSWR} was approximately 14%, 24%, and 32% as the temperature increased from 25°C to 40°C, 60°C, and 80°C. The increase for Ottawa sand [Fig. 2(f)] was approximately 15%, 34%, and 38% as temperature increased from 25°C to 40°C, 60°C, and 80°C. At the high water content of 0.3, the increase in λ^{TSWR} for Georgia kaolinite [Fig. 2(d)] was approximately 4%, 8%, and 12%; for Bonny silt [Fig. 2(e)] the increase in λ^{TSWR} was approximately 2%, 5%, and 7%; and for Ottawa sand [Fig. 2(f)] the increase in λ^{TSWR} was approximately 5%, 11%, and 15% as temperature increased from 25°C to 40°C, 60°C, and 80°C, respectively.

Effect of Elevated Temperature on Heat Transfer Mechanisms

At elevated temperatures, further considerations are needed to address the physical phenomena of the convection of pore water in both liquid and vapor phases and heat energy consumed due to phase change or latent heat transfer due to vaporization and condensation. In addition to the temperature effects on fluid properties, the thermally induced vapor diffusion in thermal conductivity formulation is considered in this section to address temperature effects on heat transfer mechanisms (i.e., conduction, convection, and latent heat flux). As the thermally induced vapor diffusion increases, the water content decreases due to the considerable amount of air voids for flow. Similar to Samarakoon and McCartney (2019), this study proposes a decay function of the degree of saturation [Fig. 1(b)] to address the increase of thermal conductivity due to the effect of elevated temperature by heat transfer mechanisms

$$\Delta\lambda^{HM} = -(\lambda_{sat} - \lambda_{dry})\frac{T - T_r}{T_r} mS \times \ln(S_{T_r}) \tag{15}$$

where S_{T_r} = degree of saturation at reference temperature. The formulation proposed by Samarakoon and McCartney (2019) requires two fitting parameters to incorporate vapor diffusion. However, no additional fitting parameters are required in the formulation proposed in this study. Furthermore, this study considers the temperature dependency of the degree of saturation, which was not accounted for in Samarakoon and McCartney (2019).

Input parameters in Table 1 were used to calculate $\Delta\lambda^{HM}$ at elevated temperatures. The sensitivity of $\Delta\lambda^{HM}$ to temperature is illustrated in Figs. 3(a–c) for Georgia kaolinite, Bonny silt, and Ottawa sand, respectively. The trend of $\Delta\lambda^{HM}$ for all three soils generally was affected by temperature-induced changes in vapor diffusion. At the reference temperature (i.e., $T = 25$°C), $\Delta\lambda^{HM}$ remained zero with changes in total water content for all three soils but exhibited nonmonotonic behavior at higher temperatures. At elevated temperatures, $\Delta\lambda^{HM}$ initially increased with total water content because the thermally induced vapor diffusion increased. For each temperature, this increasing trend continued until the funicular water content θ_f, at which the meniscus still is in a continuous state. At this point, the water content was dependent on the temperature and the type of soil [Figs. 3(a–c)]. Close to the funicular water content, the contribution of thermally-induced vapor diffusion reaches a peak as the water content decreases due to the greater availability of air-filled voids for flow. Beyond θ_f, $\Delta\lambda^{HM}$ decreases as the water content increases. As water evaporates on hot surfaces, thermally induced vapor diffusion becomes a key heat transport mechanism along with water vapor movement in wet soils. The water vapor transports the latent heat of vaporization for a unit mass of water. The flows of heat and water vapor flow are both

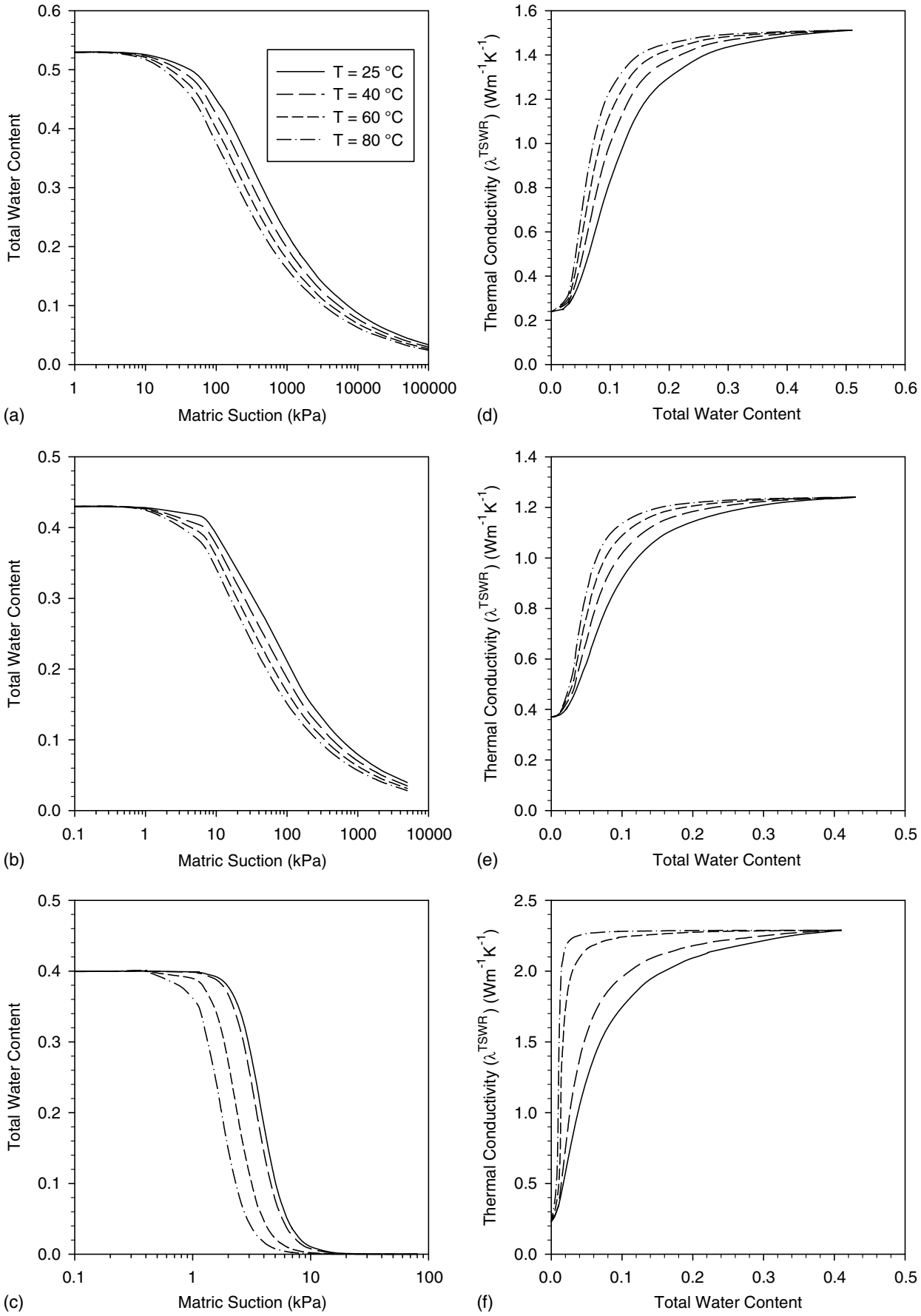

Fig. 2. SWRC and λ^{TSWR} versus total water content at different temperatures for different soils: (a and d) Georgia kaolinite; (b and e) Bonny silt; and (c and f) Ottawa sand.

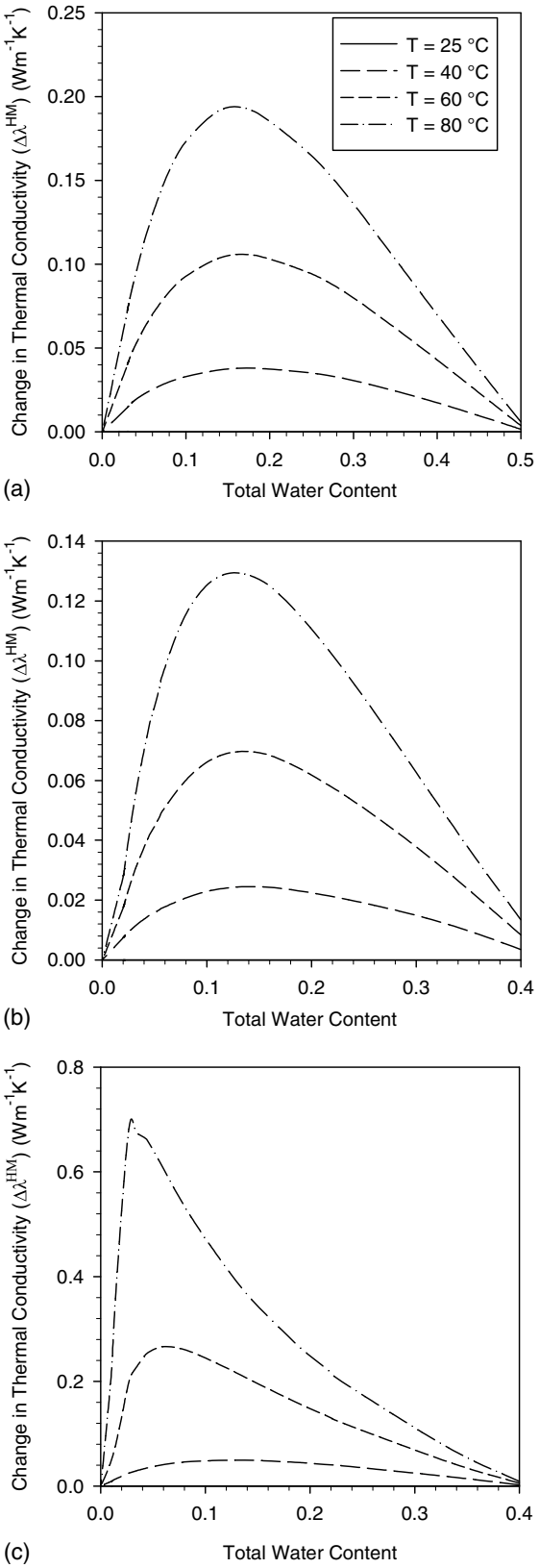

Fig. 3. Variation of $\Delta\lambda^{HM}$ with water content at different temperatures: (a) Georgia kaolinite; (b) Bonny silt; and (c) Ottawa sand.

affected by the temperature gradient in the soil. This phenomenon is prominent at high temperatures only. At low temperatures, the contribution of vapor diffusion is small, leading to a negligible latent heat component (Cass et al. 1984).

The parametric study trends in Fig. 3 are similar to the experimental data reported in the literature (Cass et al. 1984; Clutter and Ferré 2018; Xu et al. 2019). The trend of $\Delta\lambda^{HM}$ by temperature depends on the degree of saturation of the soil, which illustrates how the spaces between particles are filled. It controls the movement of water vapor and the transfer of latent heat induced under higher temperatures (Smits et al. 2013; Xu et al. 2019).

Effects of Confining Pressure on Thermal Conductivity

Confining pressure is another important parameter that affects the thermal conductivity of soils. Under an isotropic load, the soil may undergo further rearrangements of solid particles due to the reduction of interparticle shear resistance (Mitchell and Soga 2005). This may induce pore-water redistribution to balance the temporary change of suction, leading to a potential increase in thermal conductivity measurements. Another potential confinement effect is that the contact forces between soil particles increase under the application of isotropic load, which may result in a larger contact area between solid particles (Vargas and McCarthy 2001). Furthermore, the pore-water meniscus may expand due to the larger particle contact area caused by externally applied stress (Cho and Santamarina 2001). Thus, increases in isotropic net normal stresses facilitate heat passing through continuous grain–water–grain pathways.

The confinement effect is illustrated schematically in Fig. 1(c). Under unsaturated conditions, the soil mass has both air and water in the pore space. Depending on the degree of saturation, the pore air or the pore water can be either continuous or discontinuous. An increase in the confining pressure can lead to a higher packing density due to the occupancy of small particles in between the larger pore spaces that formed under lower confining pressure or stress history of the soil (Yun and Santamarina 2008). Using a set of laboratory tests, Yao et al. (2019) showed an increase in the thermal conductivity of unsaturated soils under higher confining pressures. The changes in thermal conductivity can be attributed to the pore-water redistribution and larger interface contact area of solid particles. To incorporate the effect of confining pressures into the TCF, this study proposes a new relationship as follows:

$$\Delta\lambda^{CP} = (\lambda_{sat} - \lambda_{dry}) S_{T_r} \ln\left(mf(e)\frac{(\sigma_3 - u_a)}{P_a}\right) \tag{16}$$

where $(\sigma_3 - u_a)$ = net normal stress representing net confining pressure; P_a = atmospheric pressure (~101 kPa) used as a normalizing parameter; σ_3 = total confining stress; and $f(e)$ is a function accounting for the effect of void ratio (Hardin 1978)

$$f(e) = \frac{1}{0.3 + 0.7e^2} \tag{17}$$

where e = void ratio. Hardin (1978) proposed this void ratio function to account for the rearrangement of particles due to the confining pressure for modeling the small strain shear modulus of soils. However, the same phenomenon (i.e., rearrangement of particles due to the confining pressure) is applicable and needs to be captured when modeling the TCF. Thus, the function was adopted in this study.

To illustrate the effects of confining pressure on $\Delta\lambda^{CP}$ at a constant degree of saturation, the proposed equations were employed for Georgia kaolinite, Bonny silt, and Ottawa sand. The input parameters in Table 1 were used to calculate $\Delta\lambda^{CP}$ at different confining pressures. At a constant degree of saturation $S_{T_r} = 0.2$ [Fig. 4(a)] and 0.8 [Fig. 4(b)], the changes in $\Delta\lambda^{CP}$ under different confining pressures are shown in Fig. 4 for Georgia kaolinite (solid line), Bonny silt (dashed line), and Ottawa sand (dot-dashed line), respectively. The trend was similar for both degrees of saturation

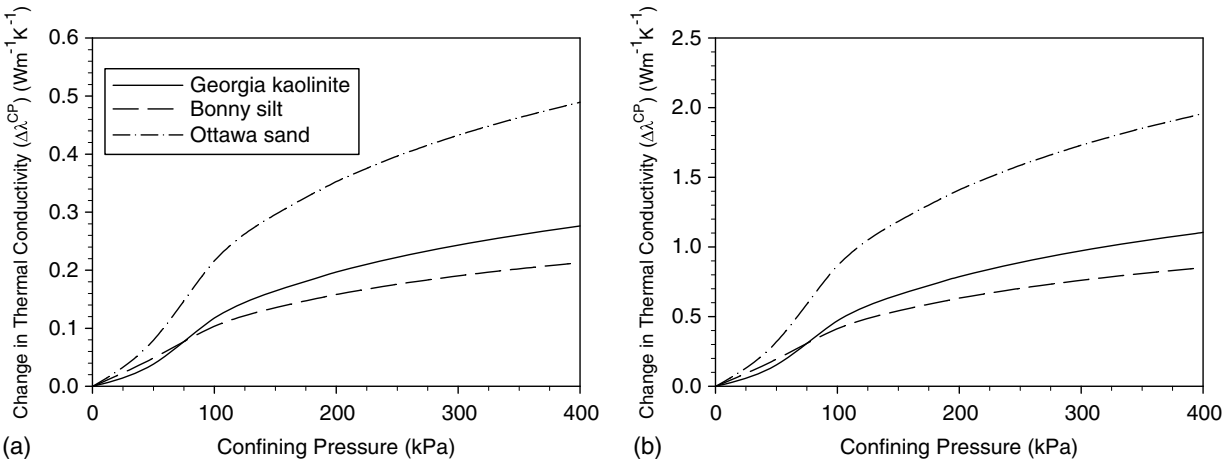

Fig. 4. Predicted $\Delta\lambda^{CP}$ versus confining pressure for Georgia kaolinite, Bonny silt, and Ottawa sand at (a) $S_{T_r} = 0.2$; and (b) $S_{T_r} = 0.8$.

considered. For all three soils, $\Delta\lambda^{CP}$ was affected by confining pressure, and increased monotonically with the confining pressure. The increase in $\Delta\lambda^{CP}$ was less pronounced for confining pressures less than the atmospheric pressure. In this range, the pore pressure generated in the soil matrix at any given degree of saturation can resist the effect of low confining pressures, leading to small changes in volumetric strain or interface contact area of solid particles. This translates into insignificant changes in the thermal conductivity of soils. Beyond P_a, the confining pressure significantly can affect the pore-water redistribution, resulting in a larger interface contact area of solid particles, implying more-significant increases in $\Delta\lambda^{CP}$.

For comparison purposes, the percentage variation of thermal conductivity was quantified for $S_{T_r} = 0.2$ at various confining pressures. The increase in $\Delta\lambda^{CP}$ for Georgia kaolinite was approximately 4%, 12%, 20%, and 24% as the confining pressure increased from 0 to 50, 100, 200, and 300 kPa. For Bonny silt, the increase in thermal conductivity was approximately 5%, 10%, 16%, and 19% as the confining pressure increased from 0 to 50, 100, 200, and 300 kPa. The increase in $\Delta\lambda^{CP}$ for Ottawa sand was approximately 8%, 22%, 35%, and 43% as the confining pressure increased from 0 to 50, 100, 200, and 300 kPa. The trends were consistent with those reported from laboratory test results in the literature (Yun and Santamarina 2008; Yao et al. 2014, 2019).

Complete Closed-Form TCF

By substituting Eqs. (13), (14), (15), and (16) into Eq. (1), the general TCF for unsaturated soils can be written as follows:

$$\lambda = \lambda_{sat} - (\lambda_{sat} - \lambda_{dry})\left[\left[1 + \left(\frac{\theta_a}{\theta_f} + \frac{(\theta_s - \theta_a)}{\theta_f}\left(1 + \left(\alpha_{VG}\psi\left(\frac{\beta_{T_r} + T_r}{\beta + T}\right)\right)^{n_{VG}}\right)^{1/n_{VG}-1}\right)^{m}\right]^{(1-m)/m} + \frac{T - T_r}{T_r} mS \times \ln(S_{T_r}) - S_{T_r}\ln\left(mf(e)\frac{(\sigma_3 - u_a)}{P_a}\right)\right] \quad (18)$$

Or, in terms of the degree of saturation

$$\lambda = \lambda_{sat} - (\lambda_{sat} - \lambda_{dry})\left[\left[1 + \left(\frac{S_a}{S_f} + \frac{(1 - S_a)}{S_f}\left(1 + (\alpha_{VG}\psi\left(\frac{\beta_{T_r} + T_r}{\beta + T}\right)\right)^{n_{VG}}\right)^{1/n_{VG}-1}\right)^{m}\right]^{(1-m)/m} + \frac{T - T_r}{T_r} mS\ln(S_{T_r}) - S_{T_r}\ln\left(mf(e)\frac{(\sigma_3 - u_a)}{P_a}\right)\right] \quad (19)$$

To illustrate the temperature dependency of the TCF under constant confining pressure, the proposed equation [Eq. (18)] was employed and studied for three different soils. Parameters in Table 1 were used to calculate the thermal conductivity of unsaturated soils. Fig. 5 shows the results for Georgia kaolinite, Bonny silt, and Ottawa sand at constant confining pressures of zero and 100 kPa. The trend of thermal conductivity for all three soils showed that it was affected by temperature-induced changes in matric suction, water content, and vapor diffusion. For Georgia kaolinite [Fig. 5(a)], Bonny silt [Fig. 5(b)], and Ottawa sand [Fig. 5(c)] at zero confining pressure, the thermal conductivity exhibited nonmonotonic behavior at relatively high temperatures ranging from 60°C to 80°C. There was an increasing trend that continued until the funicular water content θ_f, at which the water content was dependent on the temperature and type of soils [Figs. 3(a–c)]. Beyond θ_f, the thermal conductivity decreased as the water content increased. For temperatures of 25°C–40°C, the increasing trend continues for the full range of water content. Because the latent heat component is very small (Cass et al. 1984) at low temperatures, the contribution of vapor diffusion is minimal. The thermal conductivity for Ottawa sand [Fig. 5(c)] had a different trend than that of Georgia kaolinite and Bonny silt. The peak was higher and was reached at lower water

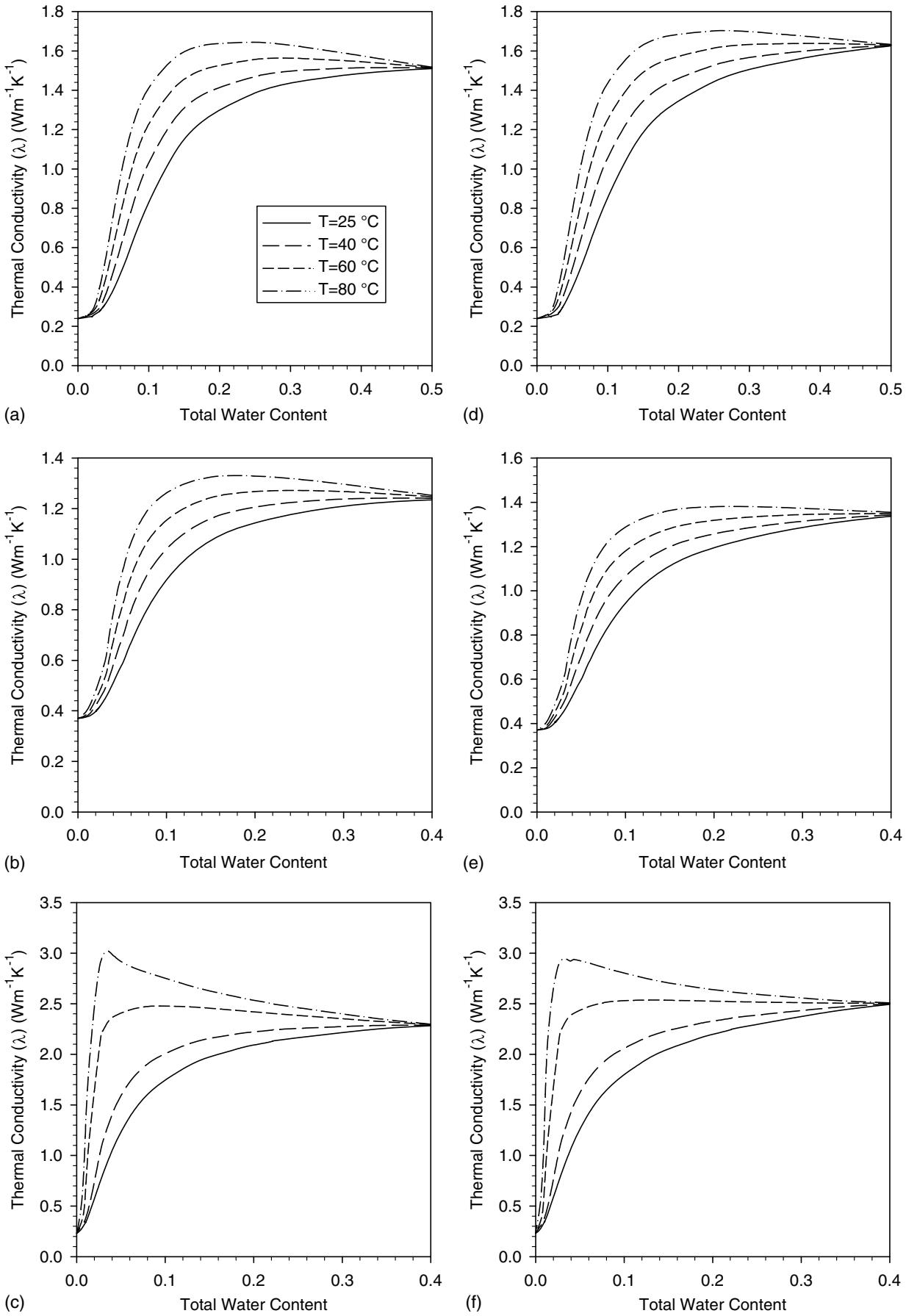

Fig. 5. Total thermal conductivity at zero and 100 kPa confining pressures under different temperatures: (a and d) Georgia kaolinite; (b and e) Bonny silt; and (c and f) Ottawa sand.

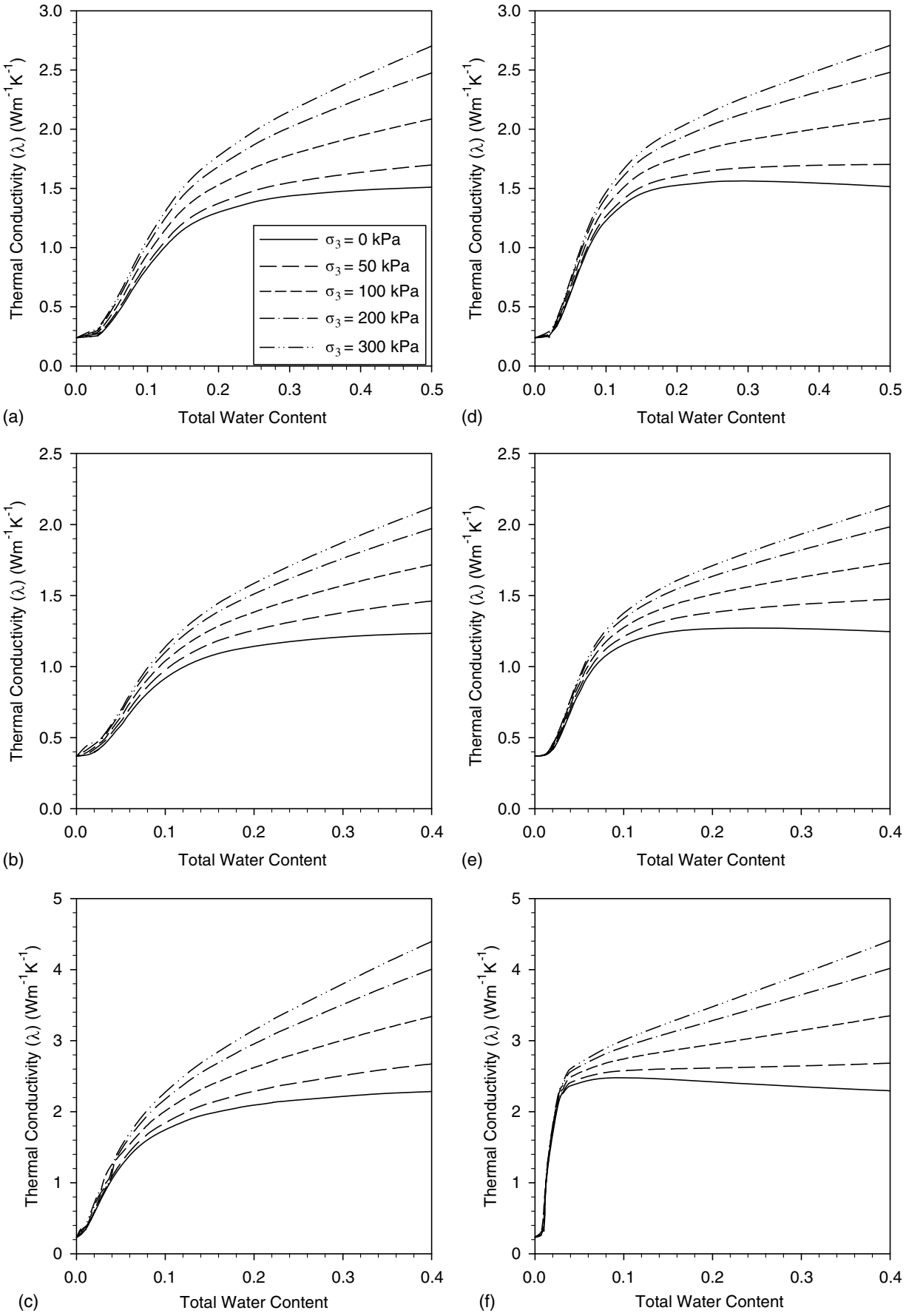

Fig. 6. Total thermal conductivity at $T = 25$°C and 60°C under different confining pressures: (a and d) Georgia kaolinite; (b and e) Bonny silt; and (c and f) Ottawa sand.

content than in the other two soils. This can be attributed to the significant impact of temperature on the menisci of the water bridges (liquid–solid) of sandy soils, which is consistent with the trend in the SWRC [Fig. 2(c)]. At low water content, increasing temperature leads to more space between particles in sand. It enhances the movement of water vapor and the transfer of latent heat due to higher temperatures and thermal gradients (Smits et al. 2013).

Under a higher confining pressure (100 kPa), there was a similar trend of the thermal conductivity versus the total water content for Georgia kaolinite [Fig. 5(d)], Bonny silt [Fig. 5(e)], and Ottawa sand [Fig. 5(f)]. However, the magnitude of thermal conductivity increased at the higher confining pressure for all soils. For example, the increase in thermal conductivity at zero confining pressure for Georgia kaolinite [Fig. 5(a)] was approximately 25%, 51%, and 74% as the temperature increased from 25°C to 40°C, 60°C, and 80°C, at a total water content of 0.1. For Bonny silt [Fig. 5(b)], the increase in thermal conductivity was approximately 9%, 21%, and 31% as the temperature increased from 25°C to 40°C, 60°C, and 80°C, at the total water content of 0.08. The increase of thermal conductivity for Ottawa sand [Fig. 5(c)] was approximately 25%, 76%, and 101% as the temperature increased from 25°C to 40°C, 60°C, and 80°C, at the total water content of 0.05. After the soil reached full saturation, thermal conductivity was closer to the value of λ_{sat}. Furthermore, the increase of thermal conductivity at the higher confining pressure (100 kPa) for Georgia kaolinite [Fig. 5(d)] was approximately 25%, 51%, and 74% as the temperature increased from 25°C to 40°C, 60°C, and 80°C, at a total water content of 0.1. For Bonny silt [Fig. 5(e)], the increase of thermal conductivity was approximately 9%, 21%, and 31% as the temperature increased from 25°C to 40°C, 60°C, and 80°C, at the total water content of 0.08. The increase of thermal conductivity for Ottawa sand [Fig. 5(f)] was approximately 25%, 76%, and 101% as the temperature increased from 25°C to 40°C, 60°C, and 80°C, at the total water content of 0.05.

The effects of confining pressure on the total thermal conductivity at a constant temperature were studied (Fig. 6). The sensitivity of total thermal conductivity to confining pressure is shown in Figs. 6(a–c) at ambient temperature (25°C) and Figs. 6(d–f) at a higher temperature (60°C) for Georgia kaolinite, Bonny silt, and Ottawa sand, respectively. For all three soils, at a given water content, the total thermal conductivity increased as the confining pressures increased from zero to 300 kPa. For each soil, the effect of confining pressure was insignificant at low water contents (<0.1) but became significant as the water content increased. For a given confining pressure, the total thermal conductivity increased as the water content increased. However, the curve reached a plateau at a certain water content for the zero confining pressure case, whereas it continued to increase monotonically at higher confining pressures. The higher the confining pressure, the more pronounced was the effect. This suggests that, at low confining pressure, the increase in thermal conductivity is dominated by the effects of temperature on water content and vapor diffusion, and confining pressure has a lesser effect. At higher confining pressures, the role of temperature in the increase of thermal conductivity is less pronounced than the contribution of confining pressure. Consequently, the behavior of thermal conductivity depends on the level of contribution from the temperature effects and the confining pressure.

The proposed TCF considers physical factors by using water content, temperature, and stress level (confining pressure) as three primary variables in the derivation. Index properties of soil are considered in the estimation of λ_{sat} and λ_{dry} [Eqs. (5)–(7)]. Furthermore, soil index properties affect the SWRC fitting parameters. Structural conditions (i.e., void ratio) are accounted for by Eqs. (16) and (17).

Validation and Comparison

The proposed TCF was compared with the experimental test results reported in the literature for Royal, Palouse A, Palouse B (Campbell et al. 1994), and Great Sand Dunes (Smits et al. 2013) at temperatures of 30°C, 50°C, and 70°C, and for Guilin lateritic clay (Xu et al. 2019) at temperatures of 25°C, 40°C, 60°C, 80°C, and 90°C. Furthermore, the predictive accuracy of the proposed TCF was compared with the following existing TCFs: Gori (1983), de Vries (1963) (two models), Tarnawski et al. (2000b), and Samarakoon and McCartney (2019). All the aforementioned laboratory tests or predictive TCFs do not consider the effect of confining pressure or set it to zero. For validation at nonzero confining pressures, the proposed TCF was compared with the results of laboratory tests reported by Yao et al. (2019) on poorly graded sand (SP4) at 20°C, 47.5°C, and 75.5°C.

The accuracy of each TCF was evaluated using the RMS error (RMSE) between the predicted and the measured data using

$$\mathrm{RMSE}(\%) = \sqrt{\frac{1}{N}\sum\left(\frac{\Theta_{\mathrm{measured}} - \Theta_{\mathrm{predicted}}}{\Theta_{\mathrm{measured}}}\right)^2} \tag{20}$$

where $\Theta_{\mathrm{measured}}$ = experimentally measured data; $\Theta_{\mathrm{predicted}}$ = predicted data from each TCF; and N = number of measured data points. For each set of data, the calibration and validation processes included two stages: (1) calibrating the TCF at ambient temperature to obtain the fitting parameters via the least-squares optimization leading to minimum error; and (2) employing the calibrated TCF to predict the thermal conductivity at elevated temperatures and comparing the result laboratory-measured data. The input SWRC and thermal parameters used for the evaluation of the proposed TCF for different soils are reported in Table 2. For comparison with the data of Yao et al. (2019), which include nonzero confining pressures, the TCF first was calibrated at ambient temperature and zero confining pressure. Then the calibrated model was used to predict the thermal conductivity at elevated temperatures and nonzero confining pressures.

Fig. 7 shows the laboratory-measured data of Campbell et al. (1994) for Royal soil and predictions of the proposed TCF at temperatures of 30°C, 50°C, and 70°C. The results obtained from the proposed models were in good agreement with the measured data. At temperatures of 30°C, 50°C, and 70°C, the RMSE values for the proposed TCF were 5.5%, 3.5%, and 7.3%, respectively. As expected, at a given degree of saturation, the thermal conductivity increased with an increase in temperature. The temperature effect was insignificant at a low degree of saturation.

Figs. 8 and 9 compare the thermal conductivity obtained from the proposed TCF with the measured data reported by Campbell et al. (1994) for Palouse A and B at various temperatures. The RMSE values of Palouse A were calculated to be 9.7%, 5.6%, and 15.4% at 30°C, 50°C, and 70°C, respectively, and those for Palouse B were 8.5%, 5.9%, and 8.5%, respectively. Fig. 10 compares the thermal conductivity obtained from the proposed TCF with the measured data of Xu et al. (2019) for Guilin lateritic clay at elevated temperatures. The RMSE values for Guilin lateritic clay were calculated to be 7.5%, 6.9%, 8.4%, 8.5%, and 8.3% at 25°C, 40°C, 60°C, 80°C, and 90°C, respectively. Overall, results obtained from the proposed model were in good agreement with the experimental results. Fig. 10 includes the measured and

Table 2. Input SWRC and thermal parameters used for evaluating the proposed TCF for different soils

Soil	SWRC parameters				TCF parameters			
	θ_s	n_{VG}	α_{VG} (kPa^{-1})	Δh_{T_r}[a] (Jm^{-2})	λ_{sat} (W m^{-1} K^{-1})	λ_{dry} (W m^{-1} K^{-1})	m	S_f
Royal[b]	0.50	6.78	0.008	−0.516	1.50	0.22	2.50	0.194
Palouse A[b]	0.53	9.67	0.002		1.37	0.20	2.82	0.237
Palouse B[b]	0.53	9.67	0.002		1.26	0.18	3.89	0.405
Great Sand Dunes[c]	0.35	4.50	0.283	−0.285	1.39	0.35	2.62	0.131
Poorly graded sand[d]	0.38	2.84	0.850		1.72	0.43	2.43	0.128
Guilin lateritic clay[e]	0.85	1.39	0.021	−0.516	1.18	0.22	2.60	0.340

[a]Reported for similar soil types by Grant and Salehzadeh (1996).
[b]Laboratory-measured thermal conductivity values reported by Campbell et al. (1994).
[c]Laboratory-measured thermal conductivity values reported by Smits et al. (2013).
[d]Laboratory-measured thermal conductivity values reported by Yao (2019).
[e]Laboratory-measured thermal conductivity values reported by Xu et al. (2019).

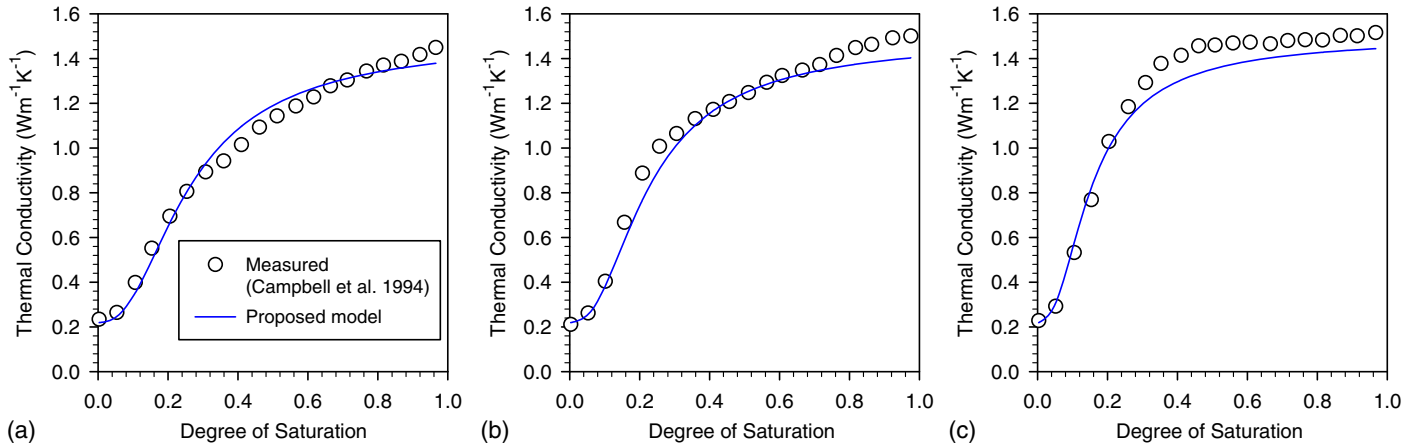

Fig. 7. Calibrated and predicted versus measured thermal conductivity for Royal soil: (a) $T = 30$°C (calibrated); (b) $T = 50$°C (predicted); and (c) $T = 70$°C (predicted).

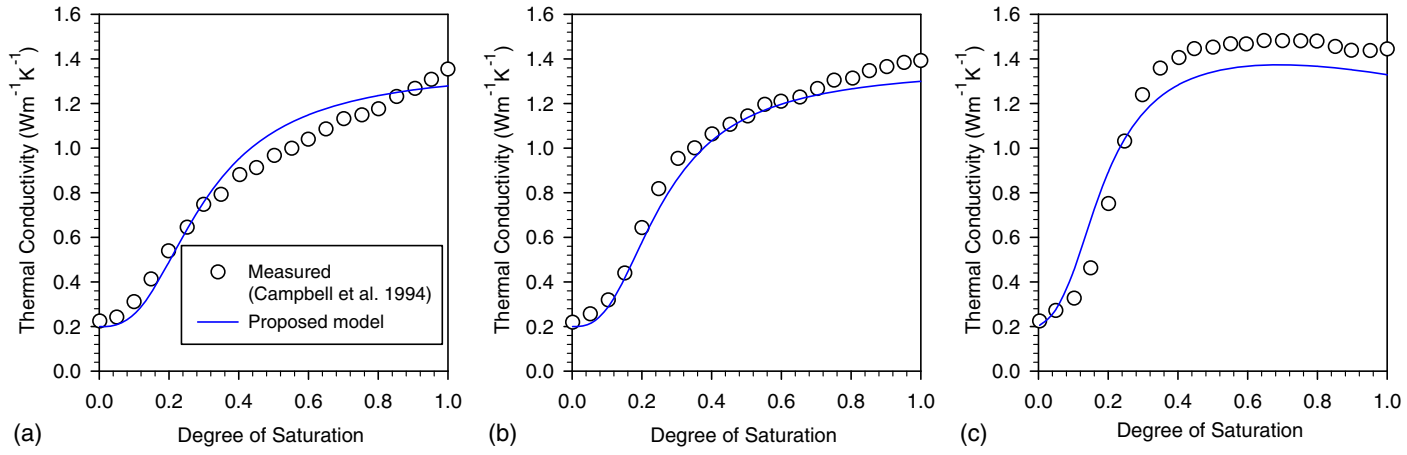

Fig. 8. Calibrated and predicted versus measured thermal conductivity for Palouse A soil: (a) $T = 30$°C (calibrated); (b) $T = 50$°C (predicted); and (c) $T = 70$°C (predicted).

predicted data up to 90°C. At such high temperatures, it was difficult to maintain an isothermal condition for the phase equilibrium of the soil sample (e.g., the high vapor pressure in a closed system). Our proposed TCF does not explicitly consider the effect of phase change and nonequilibrium conditions. However, the comparison with the laboratory test results clearly demonstrates the high predictive accuracy of the proposed model up to 90°C. This can be due to the fact that the heat transfer mechanism is incorporated, which can account for the temperature gradient (nonisothermal) and the corresponding changes in water vapor movement.

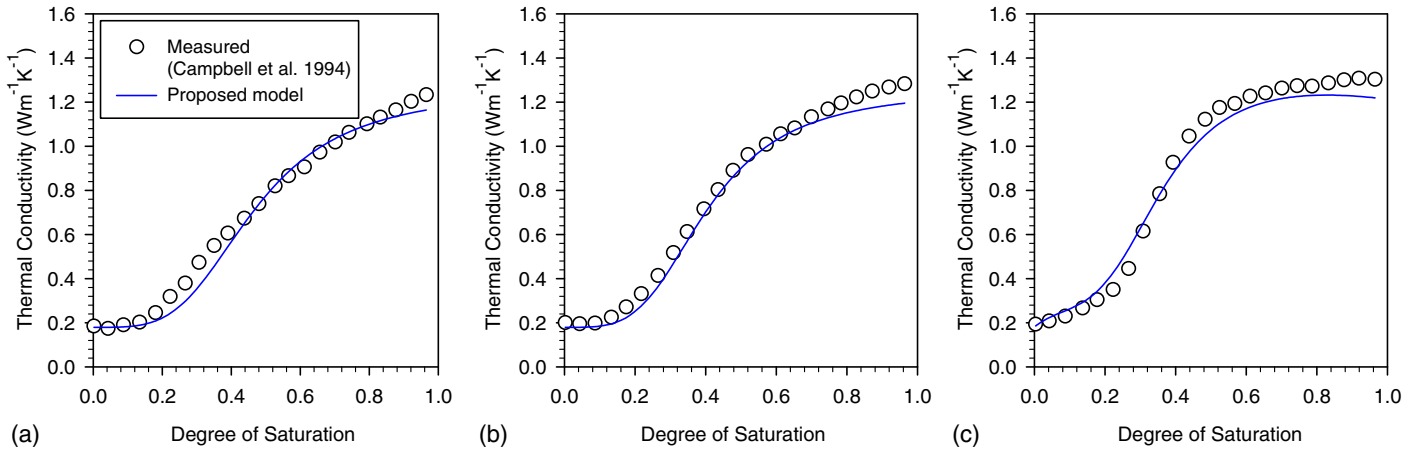

Fig. 9. Calibrated and predicted versus measured thermal conductivity for Palouse B soil: (a) $T = 30$°C (calibrated); (b) $T = 50$°C (predicted); and (c) $T = 70$°C (predicted).

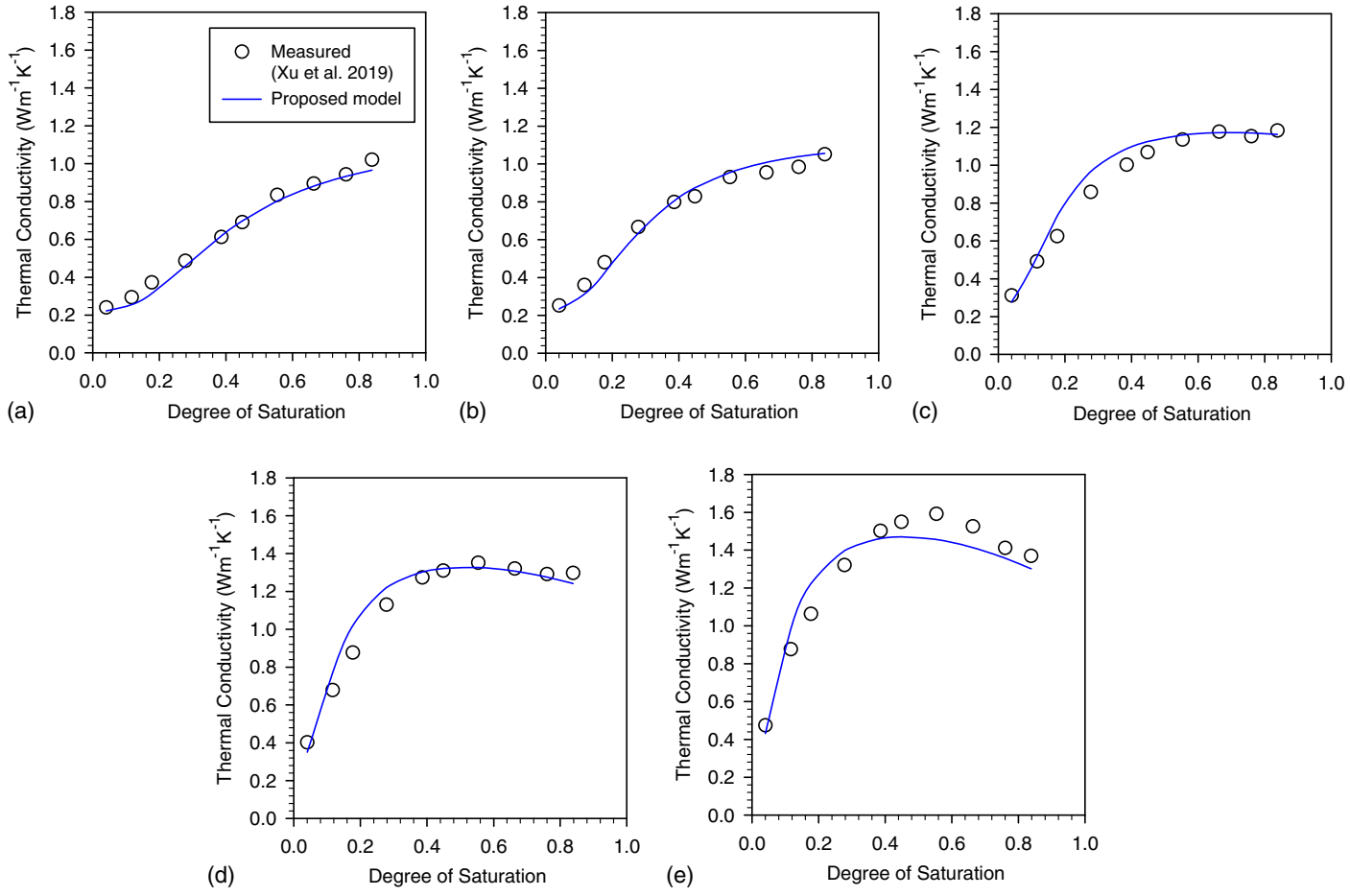

Fig. 10. Calibrated and predicted versus measured thermal conductivity for Guilin lateritic clay: (a) $T = 25$°C (calibrated); (b) $T = 40$°C (predicted); (c) $T = 60$°C (predicted); (d) $T = 80$°C (predicted); and (e) $T = 90$°C (predicted).

Fig. 11 compares the thermal conductivity from the proposed TCF with the laboratory-measured data of Smits et al. (2013) for Great Sand Dunes sand at various temperatures. The results obtained from the proposed model were in close agreement with the laboratory data. The RMSE values of Great Sand Dunes sand were calculated to be 7.6%, 7.5%, and 9.0% at 30°C, 50°C, and 70°C, respectively. To compare the performance of the proposed model with previous thermal conductivity models, the thermal conductivity formulation of Samarakoon and McCartney (2019) was used to calculate the thermal conductivity of Great Sand Dunes sand at 30°C, 50°C, and 70°C, respectively. The RMSE values of the Samarakoon and McCartney (2019) model for Great Sand Dunes sand were

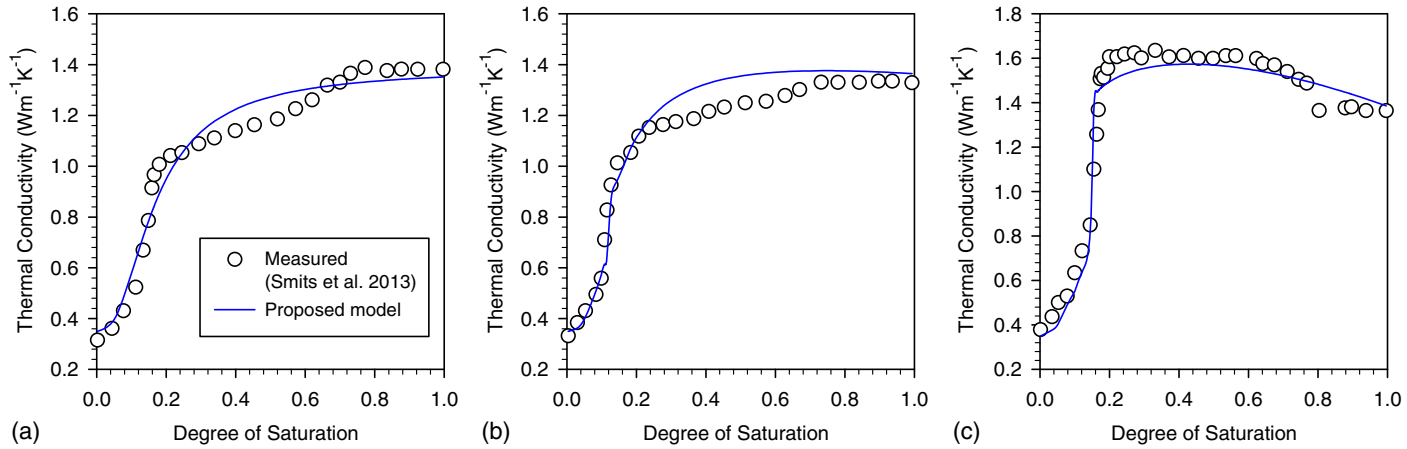

Fig. 11. Calibrated and predicted versus measured thermal conductivity for Great Sand Dunes soil: (a) $T = 30$°C (calibrated); (b) $T = 50$°C (predicted); and (c) $T = 70$°C (predicted).

Table 3. Comparison of RMSE (%) of the proposed TCF and six alternative models in predicting laboratory measure data for different soils

Soil	Temperature	Proposed model	de Vries (1963) model-1	de Vries (1963) model-2	Johansen (1975)	Gori (1983)	Tarnawski et al. (2000a)	Samarakoon and McCartney (2019)
Royal[a]	30°C	5.5	5.6	25.1	10.0	25.3	11.0	5.7
	50°C	3.5	12.0	39.0	14.3	25.6	14.0	10.2
	70°C	7.3	19.0	70.3	12.3	43.6	21.0	19.3
Palouse A[a]	30°C	9.7	6.6	16.6	10.0	28.6	12.0	9.7
	50°C	5.6	13.3	21.0	12.6	26.6	18.0	10.2
	70°C	15.4	20.0	35.0	16.3	31.3	22.0	14.0
Palouse B[a]	30°C	8.5	9.3	30.3	6.3	27.6	10.0	8.5
	50°C	5.9	10.6	36.0	6.3	29.3	19.0	13.0
	70°C	8.5	15.0	50.3	8.6	38.3	16.0	46.6
Great sand dunes[b]	30°C	7.6	—	—	—	—	—	7.6
	50°C	7.5	—	—	—	—	—	10.0
	70°C	9.0	—	—	—	—	—	15.0

Sources: Adapted from Tarnawski et al. (2000a, b).
[a]Measured data reported by Campbell et al. (1994).
[b]Measured data reported by Smits et al. (2013).

calculated to be 7.6%, 10.0%, and 15.0% at 30°C, 50°C, and 70°C, respectively. The results obtained from the proposed model clearly were in closer agreement with the experimental data than were the results of the Samarakoon and McCartney (2019) model.

Table 3 reports the RMSE values from the proposed TCF and those obtained from TCFs of de Vries (1963) (Model-1 and Model-2), Johansen (1975), Gori (1983), Tarnawski (2000a), and Samarakoon and McCartney (2019). The predictive errors are presented for five soils at various temperatures from 25°C to 90°C. The proposed TCF consistently yielded the lowest error for all soils and all temperature ranges that were examined. This superior performance can be attributed to (1) linking the TCF to a temperature-dependent SWRC model that accounts for the effects of temperature on various factors affecting water retention, and (2) accounting for thermally induced changes in heat transfer mechanisms in the proposed TCF.

To demonstrate the predictive accuracy of the proposed TCF at a given confining pressure, Fig. 12 compares the thermal conductivity from the proposed TCF with the laboratory results of Yao et al. (2019) for poorly graded sand at various temperatures and confining pressures. Because no other TCF in the literature accounts for the effect of confining pressure, no comparison was possible with alternative TCFs. The results obtained from the proposed model captured the laboratory results trend with high accuracy. The RMSE values for sand soil were calculated to be 1.6%, 2.4%, and 1.6% at 20°C, 47.5°C, and 75.5°C, respectively. The results showed that the increase of thermal conductivity was affected significantly by confining pressure due to the change in the pore-water redistribution and larger contact area with larger water meniscus between solid particles. This aspect has been overlooked in the other alternative TCFs. The effect of temperature on thermal conductivity dominated at 75.5°C for confining pressures ranging from zero to 400 kPa. The temperature effects on water content, enthalpy, and vapor diffusion were significant. These properties were less affected at lower temperatures; at 20°C and 47.5°C, the results proved that the contribution of temperature compared with that of the confining pressure was not significant.

At high temperatures (>65°C), similar behavior for all soil types was observed from the measured and predicted data. Such behavior at high temperatures can be attributed to multiple reasons. High temperatures and water contents facilitate thermally induced water movement. Furthermore, latent heat is responsible for the main part of the heat transfer at high temperatures. Another reason could be the enhancement of vapor with the variation of air-filled porosity. At high temperatures (>65°C), the vapor enhancement increases up to a certain air-filled porosity (and the corresponding volumetric water content), reaches a peak, and then decreases with further increases in air-filled porosity (and water content). The TCF exhibited the same trend at high temperatures.

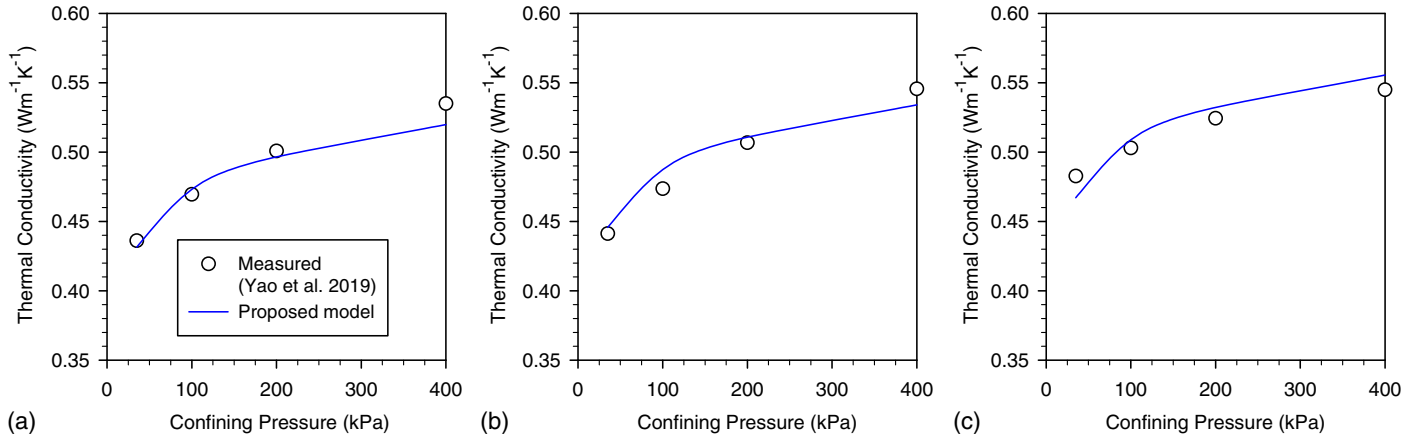

Fig. 12. Calibrated and predicted versus measured thermal conductivity for sand soil: (a) $T = 20$°C (calibrated); (b) $T = 47.5$°C (predicted); and (c) $T = 75.5$°C (predicted).

The proposed TCF offers a generalized framework to determine the thermal conductivity of unsaturated soils while accounting for the effect of water content, temperature, and confining pressure. The proposed model can be employed readily in a wide range of geotechnical and geoenvironmental engineering applications in which the thermal conductivity of unsaturated soils is needed. Elevated temperatures mean different values for different applications. Goodman and Vahedifard (2019) provided a table of several applications imposing elevated temperatures on soil, along with the pertinent range of temperature typically encountered in each application. For example, under climatic interactions, the surface temperature can reach a maximum value of about 50°C. In several near-surface geoenergy applications (e.g., energy piles, thermally active earthen systems, energy tunnels, energy diaphragm walls, and energy sheet piles), the maximum temperature imposed on the soil generally is limited to about 60°C. However, the maximum temperature can be as high as 100°C in some energy applications (e.g., nuclear waste disposal and buried high-voltage cables). In some geoenvironmental engineering applications, thermal interactions (e.g., smoldering combustion and remediation) can lead to extremely high temperatures (several hundred degrees). In this paper, we validated the proposed TCF with laboratory-measured data up to 90°C, which covers the maximum temperature involved in several of the aforementioned applications. For temperatures higher than those studied in this paper, further studies are recommended to extend the proposed TCF by considering additional factors (e.g., phase change, nonequilibrium, and the effect of temperature on solid grains). Furthermore, elevated temperatures possibly can induce desiccation cracks in clayey soils. Previous studies (Tang et al. 2008; 2010; Salimi et al. 2021a, b) have shown that elevated temperatures decrease the tensile strength of unsaturated soils and form cracks at higher rates. The formation of cracks can undermine the integrity of unsaturated earthen structures and slopes (Abdollahi et al. 2021), and also can alter heat transfer and water retention mechanisms in the soil. The proposed TCF in this study was developed for intact soils. However, the TCF can be extended in future studies to consider the role of temperature in crack formation and the subsequent changes in heat transfer and water retention mechanisms of cracked unsaturated soils.

Conclusions

Considering the effects of temperature and confining pressure on thermal conductivity is an important step toward accurate modeling of the unsaturated soil behavior, particularly when dealing with applications that involve elevated temperatures in unsaturated soils. This study presented a generalized TCF to determine the thermal conductivity of unsaturated soils while accounting for the effect of various water content (or suction), temperature, and confining pressures. Under elevated temperature and confining pressure conditions, a direct link was presented between the soil water retention curve, different heat transfer mechanisms (i.e., conduction, convection, and latent heat flux), and the confining pressure with the thermal conductivity formulation for unsaturated soils.

Employing the proposed TCF, parametric studies were conducted to gain further insight into the effect of temperatures on water content and thermal conductivity at constant confining pressure for three different soils. The effects of confining pressures at a constant temperature on thermal conductivity also were studied. Different behaviors of thermal conductivity were observed depending upon the type of soil, range of temperature, water content, and confining pressure. Finally, predictions from the proposed TCF were compared with and validated against experimental data for six different soils from the literature. Results obtained from the proposed model were more accurate and were in closer agreement with laboratory-measured data than were the results of several existing TCFs. The error for all soils at various temperatures consistently was less than 10%. The proposed TCF can be considered as a generalized framework describing the thermal conductivity of unsaturated soils under different temperature and confining pressure conditions. The findings of this study can be used to improve the modeling of thermal conductivity in applications in which temperature and confining pressure changes are expected in unsaturated soils.

Data Availability Statement

All data, models, and code generated or used during the study appear in the published article.

Acknowledgments

This material is based upon work supported in part by the National Science Foundation (NSF) under Grant No. CMMI-1634748 and the US Army Engineer Research and Development Center (ERDC) under contract W912HZ19C0036. The views and conclusions contained herein are those of the authors and should not be interpreted

as necessarily representing the official policies or endorsements, either expressed or implied, of NSF, ERDC, or the US Government. Distribution Statement A: Approved for public release: distribution unlimited.

References

Abdollahi, M., F. Vahedifard, M. Abed, and B. A. Leshchinsky. 2021. "Effect of tension crack formation on active earth pressures encountered in unsaturated retaining wall backfills." *J. Geotech. Geoenviron. Eng.* 147 (2): 06020028. https://doi.org/10.1061/(ASCE)GT.1943-5606.0002434.

Aduda, B. O. 1996. "Effective thermal conductivity of loose particulate systems." *J. Mater. Sci.* 31 (24): 6441–6448. https://doi.org/10.1007/BF00356246.

Alsherif, N. A., and J. S. McCartney. 2015. "Thermal behaviour of unsaturated silt at high suction magnitudes." *Géotechnique* 65 (9): 703–716. https://doi.org/10.1680/geot.14.P.049.

Brandon, T. L., and J. K. Mitchell. 1989. "Factors influencing thermal resistivity of sands." *J. Geotech. Eng.* 115 (12): 1683–1698. https://doi.org/10.1061/(ASCE)0733-9410(1989)115:12(1683).

Campbell, G. S., J. D. Jungbauer Jr., W. R. Bidlake, and R. D. Hungerford. 1994. "Predicting the effect of temperature on soil thermal conductivity." *Soil Sci.* 158 (5): 307–313. https://doi.org/10.1097/00010694-199411000-00001.

Cass, A., G. S. Campbell, and T. L. Jones. 1984. "Enhancement of thermal water vapor diffusion in soil." *Soil Sci. Soc. Am. J.* 48 (1): 25–32. https://doi.org/10.2136/sssaj1984.03615995004800010005x.

Chen, S. X. 2008. "Thermal conductivity of sands." *Heat Mass Transfer* 44 (10): 1241–1246. https://doi.org/10.1007/s00231-007-0357-1.

Cho, G. C., and J. C. Santamarina. 2001. "Unsaturated particulate materials—Particle-level studies." *J. Geotech. Geoenviron. Eng.* 127 (1): 84–96. https://doi.org/10.1061/(ASCE)1090-0241(2001)127:1(84).

Clutter, M., and T. P. A. Ferré. 2018. "Examining the potentials and limitations of using temperature tracing to infer water flux through unsaturated soils." *Vadose Zone J.* 17 (1): 1–8. https://doi.org/10.2136/vzj2017.10.0181.

Coccia, C. J. R., and J. S. McCartney. 2012. "A thermo-hydro-mechanical true triaxial cell for evaluation of the impact of anisotropy on thermally-induced volume changes in soils." *ASTM Geotech. Test. J.* 35 (2): 227–237. https://doi.org/10.1520/GTJ103803.

Cortes, D. D., A. I. Martin, T. S. Yun, F. M. Francisca, J. C. Santamarina, and C. Ruppel. 2009. "Thermal conductivity of hydrate-bearing sediments." *J. Geophy. Res. Solid Earth* 114 (B11): B11103. https://doi.org/10.1029/2008JB006235.

Côté, J., and J.-M. Konrad. 2005. "A generalized thermal conductivity model for soils and construction materials." *Can. Geotech. J.* 42 (2): 443–458. https://doi.org/10.1139/t04-106.

de Vries, D. A. 1963. "Thermal properties of soils." In *Physics of plant environment*, edited by W. R. Van Wijk, 210–235. New York: Wiley.

Dong, Y., J. S. McCartney, and N. Lu. 2015. "Critical review of thermal conductivity models for unsaturated soils." *Geotech. Geol. Eng.* 33 (2): 207–221. https://doi.org/10.1007/s10706-015-9843-2.

Ebigbo, A. 2005. "Thermal effects of carbon dioxide sequestration in the subsurface." Doctoral dissertation, Institut für Wasserbau, Universität Stuttgart.

Esch, D. C. 2004. *Thermal analysis, construction, and monitoring methods for frozen ground*. Reston, VA: ASCE.

Everett, D. H. 1972. "Manual of symbols and terminology for physicochemical quantities and units, Appendix II: Definitions, terminology and symbols in colloid and surface chemistry." *Pure Appl. Chem.* 31 (4): 577–638. https://doi.org/10.1351/pac197231040577.

Gangadhara Rao, M. V. B. B., and D. N. Singh. 1999. "A generalized relationship to estimate thermal resistivity of soils." *Can. Geotech. J.* 36 (4): 767–773. https://doi.org/10.1139/t99-037.

Goodman, C. C., and F. Vahedifard. 2019. "Micro-scale characterisation of clay at elevated temperatures." *Géotechnique Lett.* 9 (3): 225–230. https://doi.org/10.1680/jgele.19.00026.

Gori, F. 1983. "A theoretical model for predicting the effective thermal conductivity of unsaturated frozen soils." In *Proc., 4th Int. Conf. on Permafrost*, 363–368. Washington, DC: National Academy Press.

Gori, F., and S. Corasaniti. 2002. "Theoretical prediction of the soil thermal conductivity at moderately high temperatures." *J. Heat Transfer* 124 (6): 1001–1008. https://doi.org/10.1115/1.1513573.

Grant, S. A., and A. Salehzadeh. 1996. "Calculation of temperature effects on wetting coefficients of porous solids and their capillary pressure functions." *Water Resour. Res.* 32 (2): 261–270. https://doi.org/10.1029/95WR02915.

Haigh, S. K. 2012. "Thermal conductivity of sands." *Géotechnique* 62 (7): 617–625. https://doi.org/10.1680/geot.11.P.043.

Hardin, B. O. 1978. "The nature of stress-strain behavior for soils." In Vol. 1 of *Proc., ASCE Geotechnical Engineering Division Specialty Conf. on Earthquake Engineering and Soil Dynamics*, 1–90. Reston, VA: ASCE.

Hiraiwa, Y., and T. Kasubuchi. 2000. "Temperature dependence of thermal conductivity of soil over a wide range of temperature (5–75°C)." *Eur. J. Soil Sci.* 51 (2): 211–218. https://doi.org/10.1046/j.1365-2389.2000.00301.x.

Hu, X.-J., J.-H. Du, S.-Y. Lei, and B.-X. Wang. 2001. "A model for the thermal conductivity of unconsolidated porous media based on capillary pressure-saturation relation." *Int. J. Heat Mass Transfer* 44 (1): 247–251. https://doi.org/10.1016/S0017-9310(00)00079-X.

Jin, H., Y. Wang, Q. Zheng, H. Liu, and E. Chadwick. 2017. "Experimental study and modelling of the thermal conductivity of sandy soils of different porosities and water contents." *Appl. Sci.* 7 (2): 119. https://doi.org/10.3390/app7020119.

Johansen, O. 1975. "Thermal conductivity of soils." Ph.D. dissertation, Defense Technical Information Center, Norwegian Univ. of Science and Technology.

Kasubuchi, T. 1992. "Development of in-situ soil water measurement by heat-probe method." *JARQ (Japan)* 26 (3): 178–181.

Kasubuchi, T., and S. Hasegawa. 1994. "Measurement of spatial average of field soil water content by the long heat probe method." *Soil Sci. Plant Nutr.* 40 (4): 565–571. https://doi.org/10.1080/00380768.1994.10414295.

Lu, N. 2016. "Generalized soil water retention equation for adsorption and capillarity." *J. Geotech. Geoenviron. Eng.* 142 (10): 04016051. https://doi.org/10.1061/(ASCE)GT.1943-5606.0001524.

Lu, N., and Y. Dong. 2015. "Closed-form equation for thermal conductivity of unsaturated soils at room temperature." *J. Geotech. Geoenviron. Eng.* 141 (6): 04015016. https://doi.org/10.1061/(ASCE)GT.1943-5606.0001295.

Lu, N., and S. Ge. 1996. "Effect of horizontal heat and fluid flow on the vertical temperature distribution in a semiconfining layer." *Water Resour. Res.* 32 (5): 1449–1453. https://doi.org/10.1029/95WR03095.

Lu, N., and W. J. Likos. 2004. *Unsaturated soil mechanics*. New York: Wiley.

Lu, N., and W. J. Likos. 2006. "Suction stress characteristic curve for unsaturated soil." *J. Geotech. Geoenviron. Eng.* 132 (2): 131–142. https://doi.org/10.1061/(ASCE)1090-0241(2006)132:2(131).

Lu, S., T. Ren, Y. Gong, and R. Horton. 2007. "An improved model for predicting soil thermal conductivity from water content at room temperature." *Soil Sci. Soc. Am. J.* 71 (1): 8–14. https://doi.org/10.2136/sssaj2006.0041.

McCartney, J. S., C. J. R. Coccia, N. Alsherif, and M. A. Stewart. 2013. "Energy geostructures in unsaturated soils." In *Energy geo-structures: Innovation in underground engineering*, edited by L. Laloui and A. DiDonna, 99–114. Hoboken, NJ: Wiley.

McCartney, J. S., N. H. Jafari, T. Hueckel, M. Sanchez, and F. Vahedifard. 2019. "Emerging thermal issues in geotechnical engineering." In *Geotechnical fundamentals for addressing new world challenges*, edited by N. Lu and J. K. Mitchell, 275–317. Berlin: Springer.

Mitchell, J. K., and K. Soga. 2005. *Fundamentals of soil behavior*. New York: Wiley.

Moradi, A., K. M. Smits, N. Lu, and J. S. McCartney. 2016. "Heat transfer in unsaturated soil with application to borehole thermal energy storage." *Vadose Zone J.* 15 (10): 16. https://doi.org/10.2136/vzj2016.03.0027.

Preene, M., and W. Powrie. 2009. "Ground energy systems: From analysis to geotechnical design." *Géotechnique* 59 (3): 261–271. https://doi.org/10.1680/geot.2009.59.3.261.

Robinson, J. D., and F. Vahedifard. 2016. "Weakening mechanisms imposed on California's levees under multiyear extreme drought." *Clim. Change* 137 (1): 1–14. https://doi.org/10.1007/s10584-016-1649-6.

Sahimi, M., and T. T. Tsotsis. 1997. "Transient diffusion and conduction in heterogeneous media: Beyond the classical effective-medium approximation." *Ind. Eng. Chem. Res.* 36 (8): 3043–3052. https://doi.org/10.1021/ie960602k.

Salimi, K., A. Cerato, F. Vahedifard, and G. Miller. 2021a. "Tensile strength of compacted clays during desiccation under elevated temperatures." *Geotech. Test. J.* 44 (4): 12. https://doi.org/10.1520/GTJ20200114.

Salimi, K., A. Cerato, F. Vahedifard, and G. A. Miller. 2021b. "A temperature-dependent model for tensile strength characteristic curve of unsaturated soils." *Geomech. Energy Environ.* 28 (Dec): 100244. https://doi.org/10.1016/j.gete.2021.100244.

Samarakoon, R. A., and J. S. McCartney. 2019. "Simplified model for heat transfer in unsaturated soils considering a nonisothermal thermal conductivity function." *Geotech. Eng. J.* 50 (1): 16–22.

Slavin, A. J., F. A. Londry, and J. Harrison. 2000. "A new model for the effective thermal conductivity of packed beds of solid spheroids: Alumina in helium between 100 and 500°C." *Int. J. Heat Mass Transfer* 43 (Jun): 2059–2073. https://doi.org/10.1016/S0017-9310(99)00290-2.

Smith, W. O. 1942. "The thermal conductivity of dry soil." *Soil Sci.* 53 (6): 435–460. https://doi.org/10.1097/00010694-194206000-00003.

Smits, K. M., T. Sakaki, S. E. Howington, J. F. Peters, and T. H. Illangasekare. 2013. "Temperature dependence of thermal properties of sands over a wide range of temperatures (30–70°C)." *Vadose Zone J.* 12 (1): 33. https://doi.org/10.2136/vzj2012.0033.

Tang, C., B. Shi, C. Liu, L. Zhao, and B. Wang. 2008. "Influencing factors of geometrical structure of surface shrinkage cracks in clayey soils." *Eng. Geol.* 101 (3–4): 204–217. https://doi.org/10.1016/j.enggeo.2008.05.005.

Tang, C.-S., Y.-J. Cui, A.-M. Tang, and B. Shi. 2010. "Experiment evidence on the temperature dependence of desiccation cracking behavior of clayey soils." *Eng. Geol.* 114 (3–4): 261–266. https://doi.org/10.1016/j.enggeo.2010.05.003.

Tarnawski, V. R., F. Gori, B. Wagner, and G. D. Buchan. 2000a. "Modeling Approaches to predicting thermal conductivity of soils at high temperatures." *Int. J. Energy Res.* 24 (5): 403–423. https://doi.org/10.1002/(SICI)1099-114X(200004)24:5<403::AID-ER588>3.0.CO;2-#.

Tarnawski, V. R., W. H. Leong, and K. L. Bristow. 2000b. "Developing a temperature-dependent Kersten function for soil thermal conductivity." *Int. J. Energy Res.* 24 (15): 1335–1350. https://doi.org/10.1002/1099-114X(200012)24:15<1335::AID-ER652>3.0.CO;2-X.

Tarnawski, V. R., M. L. McCombie, T. Momose, I. Sakaguchi, and W. H. Leong. 2013. "Thermal conductivity of standard sands. Part III. Full range of saturation." *Int. J. Thermophys.* 34 (Apr): 1130–1147. https://doi.org/10.1007/s10765-013-1455-6.

Tarnawski, V. R., T. Momose, and W. H. Leong. 2009. "Assessing the impact of quartz content on the prediction of soil thermal conductivity." *Géotechnique* 59 (4): 331–338. https://doi.org/10.1680/geot.2009.59.4.331.

Vahedifard, F., A. AghaKouchak, and N. H. Jafari. 2016a. "Compound hazards yield Louisiana flood." *Science* 353 (6306): 1374. https://doi.org/10.1126/science.aai8579.

Vahedifard, F., A. AghaKouchak, E. Ragno, S. Shahrokhabadi, and I. Mallakpour. 2017. "Lessons from the Oroville Dam." *Science* 355 (6330): 1139–1140. https://doi.org/10.1126/science.aan0171.

Vahedifard, F., T. D. Cao, E. Ghazanfari, and S. K. Thota. 2019. "Closed-form models for nonisothermal effective stress of unsaturated soils." *J. Geotech. Geoenviron. Eng.* 145 (9): 04019053. https://doi.org/10.1061/(ASCE)GT.1943-5606.0002094.

Vahedifard, F., T. D. Cao, S. K. Thota, and E. Ghazanfari. 2018. "Nonisothermal models for soil–water retention curve." *J. Geotech. Geoenviron. Eng.* 144 (9): 04018061. https://doi.org/10.1061/(ASCE)GT.1943-5606.0001939.

Vahedifard, F., J. D. Robinson, and A. AghaKouchak. 2016b. "Can protracted drought undermine the structural integrity of California's earthen levees?" *J. Geotech. Geoenviron. Eng.* 142 (6): 02516001. https://doi.org/10.1061/(ASCE)GT.1943-5606.0001465.

Vahedifard, F., S. K. Thota, T. C. Cao, R. A. Samarakoon, and J. S. McCartney. 2020. "A temperature-dependent model for small-strain shear modulus of unsaturated soils." *J. Geotech. Geoenviron. Eng.* 146 (12): 04020136. https://doi.org/10.1061/(ASCE)GT.1943-5606.0002406.

van Genuchten, M. T. 1980. "A closed-form equation for predicting the hydraulic conductivity of unsaturated soils." *Soil Sci. Soc. Am. J.* 44 (5): 892–898. https://doi.org/10.2136/sssaj1980.03615995004400050002x.

Vargas, W. L., and J. J. McCarthy. 2001. "Heat conduction in granular materials." *AIChE J.* 47 (5): 1052–1059. https://doi.org/10.1002/aic.690470511.

Wallen, B. M., K. M. Smits, T. Sakaki, S. E. Howington, and T. K. K. C. Deepagoda. 2016. "Thermal conductivity of binary sand mixtures evaluated through full water content range." *Soil Sci. Soc. Am. J.* 80 (3): 592–603. https://doi.org/10.2136/sssaj2015.11.0408.

Watson, K. M. 1943. "Thermodynamics of the liquid state." *Ind. Eng. Chem.* 35 (4): 398–406. https://doi.org/10.1021/ie50400a004.

Xu, L., W. M. Ye, B. Chen, Y. G. Chen, and Y. J. Cui. 2016. "Experimental investigations on thermo-hydro-mechanical properties of compacted GMZ01 bentonite-sand mixture using as buffer materials." *Eng. Geol.* 213 (81): 46–54. https://doi.org/10.1016/j.enggeo.2016.08.015.

Xu, Y., D. Sun, Z. Zeng, and H. Lv. 2019. "Effect of temperature on thermal conductivity of lateritic clays over a wide temperature range." *Int. J. Heat Mass Transfer* 138 (Jan): 562–570. https://doi.org/10.1016/j.ijheatmasstransfer.2019.04.077.

Yao, J., H. Oh, W. J. Likos, and J. M. Tinjum. 2014. "Three laboratory methods for measuring thermal resistivity dryout curves of coarse-grained soils." *Geotech. Test. J.* 37 (6): 20140120. https://doi.org/10.1520/GTJ20140120.

Yao, J., T. Wang, and W. J. Likos. 2019. "Measuring thermal conductivity of unsaturated sand under different temperatures and stress levels using a suction-controlled thermo-mechanical method." In *Geo-congress 2019: Geotechnical materials, modeling, and testing*, 784–793. Reston, VA: ASCE.

Yun, T. S., and J. C. Santamarina. 2008. "Fundamental study of thermal conduction in dry soils." *Granular Matter* 10 (3): 197. https://doi.org/10.1007/s10035-007-0051-5.

Zhang, N., and Z. Wang. 2017. "Review of soil thermal conductivity and predictive models." *Int. J. Therm. Sci.* 117 (21): 172–183. https://doi.org/10.1016/j.ijthermalsci.2017.03.013.

Zhang, T., G. Cai, S. Liu, and A. J. Puppala. 2017. "Investigation on thermal characteristics and prediction models of soils." *Int. J. Heat Mass Transfer* 106 (3): 1074–1086. https://doi.org/10.1016/j.ijheatmasstransfer.2016.10.084.

Zhang, Y., N. Lu, and B. Ross. 1994. "Convective instability of moist gas in a porous medium." *Int. J. Heat Mass Transfer* 37 (1): 129–138. https://doi.org/10.1016/0017-9310(94)90167-8.